Meteorología del Espacio (Space Weather)

Tercera Reunión sobre Proyectos del Programa MET del GREPECAS para la Región SAM

Lic. Vanina Lanabere vlanabere@at.fcen.uba.ar

Departamento de Ciencias de la Atmósfera y los Océanos,
Universidad de Buenos Aires (UBA), Argentina

Dr. Sergio Dasso sdasso@iafe.uba.ar

Instituto de Astronomía y Física del Espacio - UBA-CONICET
Departamento de Ciencias de la Atmósfera y los Océanos,
UBA, Argentina
Departamento de Física - UBA- Argentina

Laboratorio Argentino de Meteorología del esPacio

www.iafe.uba.ar/u/lamp

17 de Junio de 2019

PART II: Space Weather Impacts

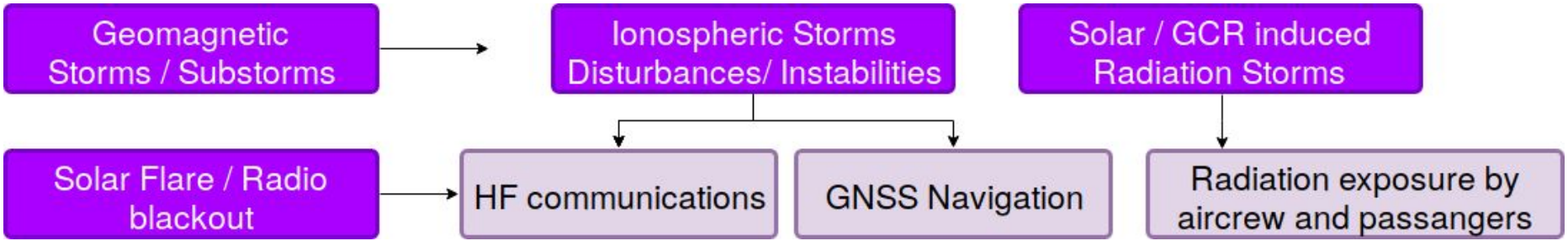

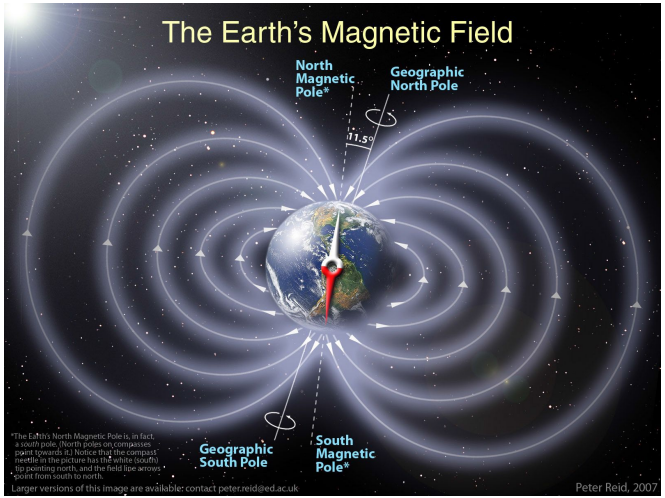

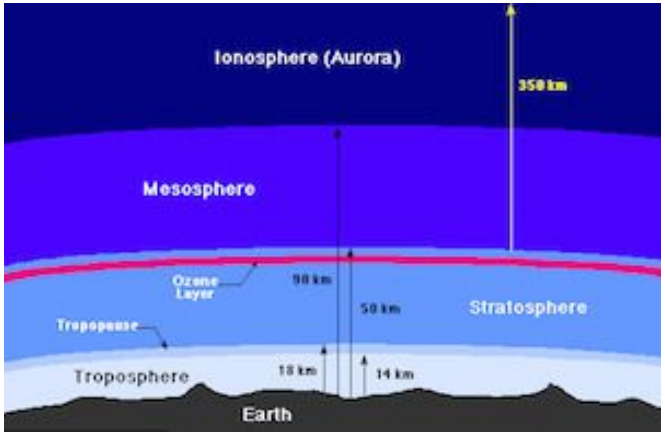

The geomagnetic field

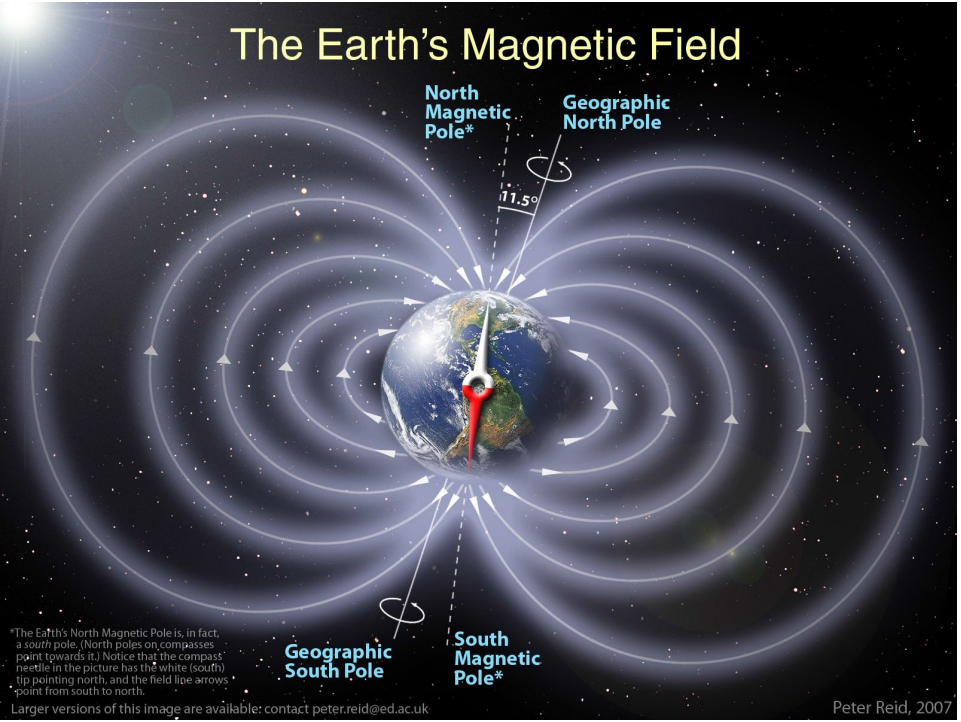

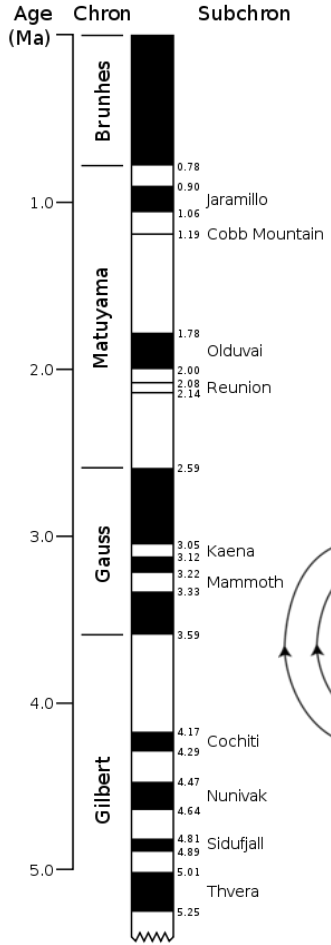

There have been 183 reversals over the last 83 million years

The latest, The Brunhes–Matuyama reversal, occurred 780,000 years ago

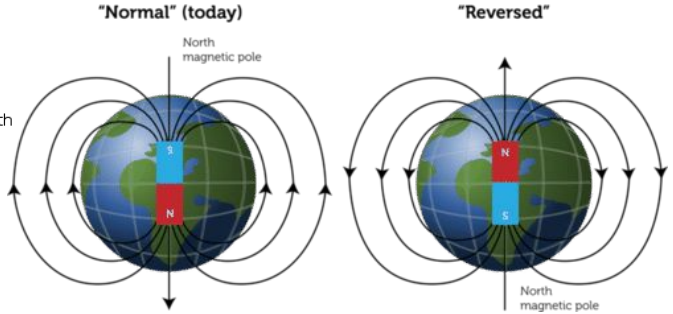

Magnetic field components

Intensity parameters

Horizontal intensity (H)
Vertical intensity (Z)
Total intensity (F)
The north (X) and
east (Y) components of the horizontal

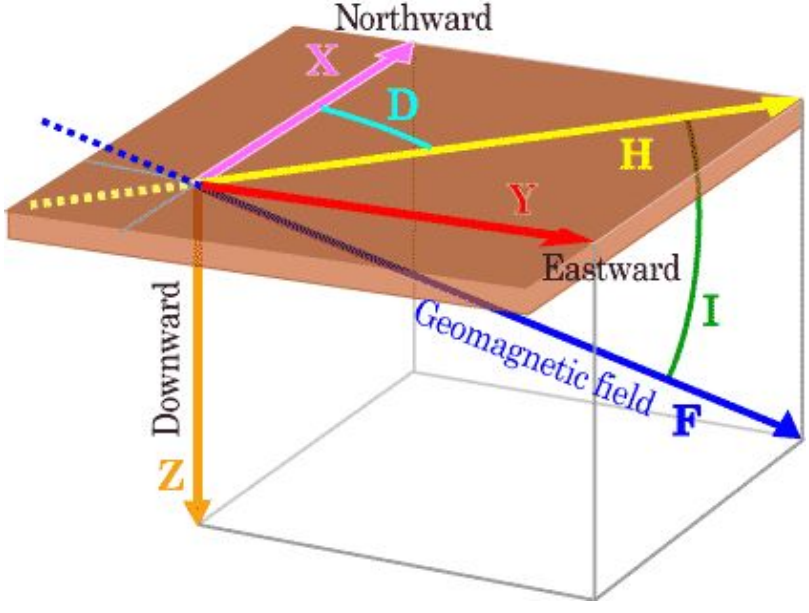

Direction parameters

Declination (D) is considered positive when measured east of north

Inclination (I) and vertical intensity (Z) positive down

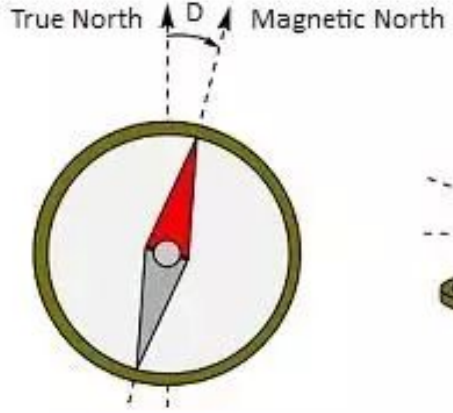

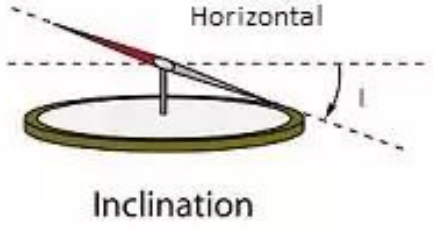

US/UK World Magnetic Model - Epoch 2015.0
Main Field Total Intensity (F)

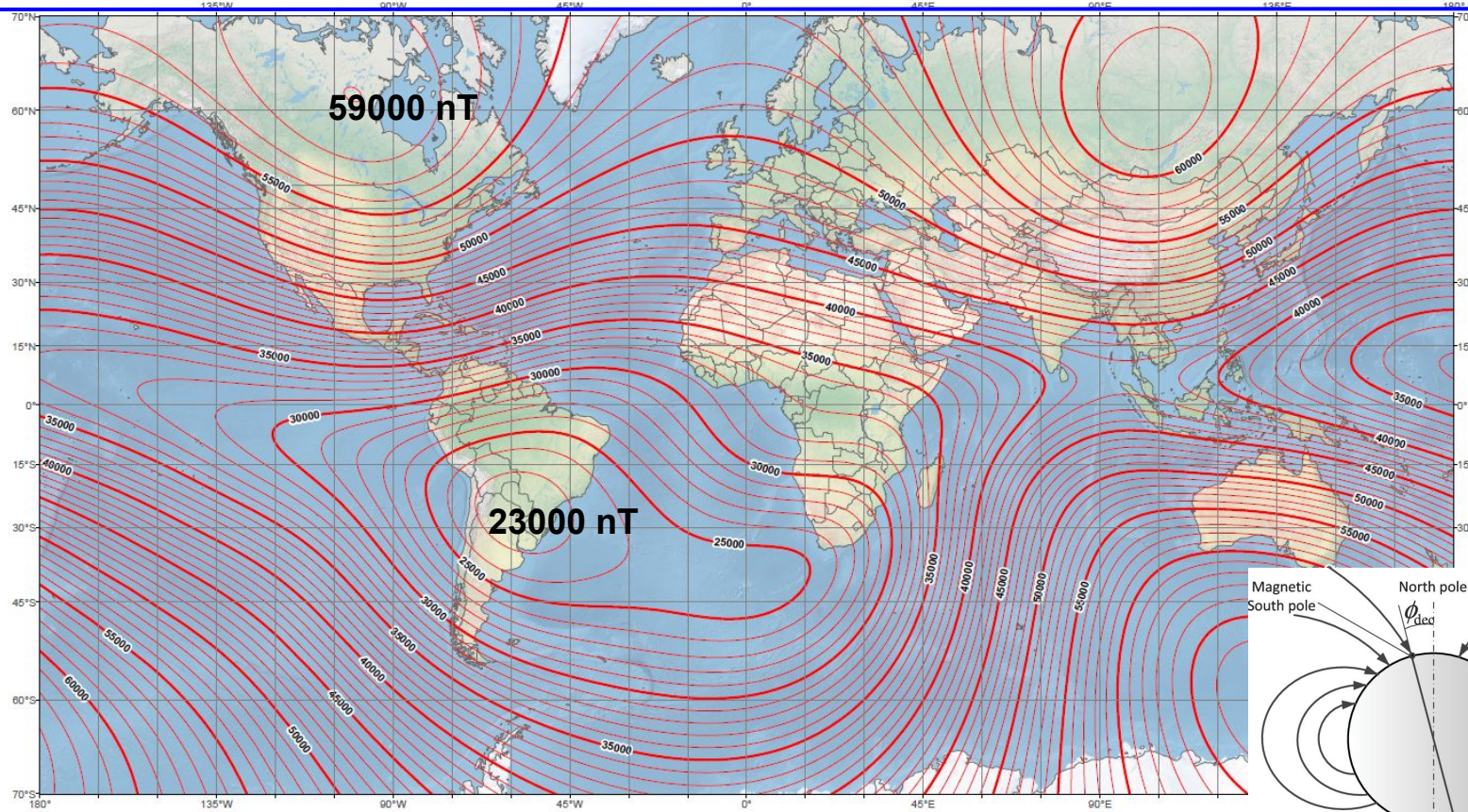

Main Field Total Intensity (F)
Contour interval: 1000 nT.
Mercator Projection.
: Position of dip poles

Map developed by NOAA/N
http://ngdc.noaa.gov/geom
Map reviewed by NGA and B
Published December 2014

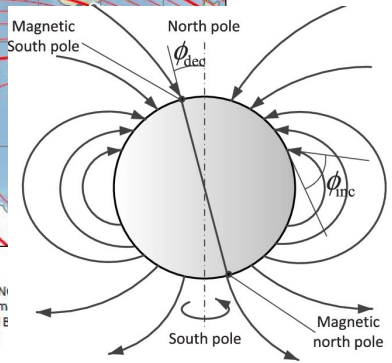

Secular variation

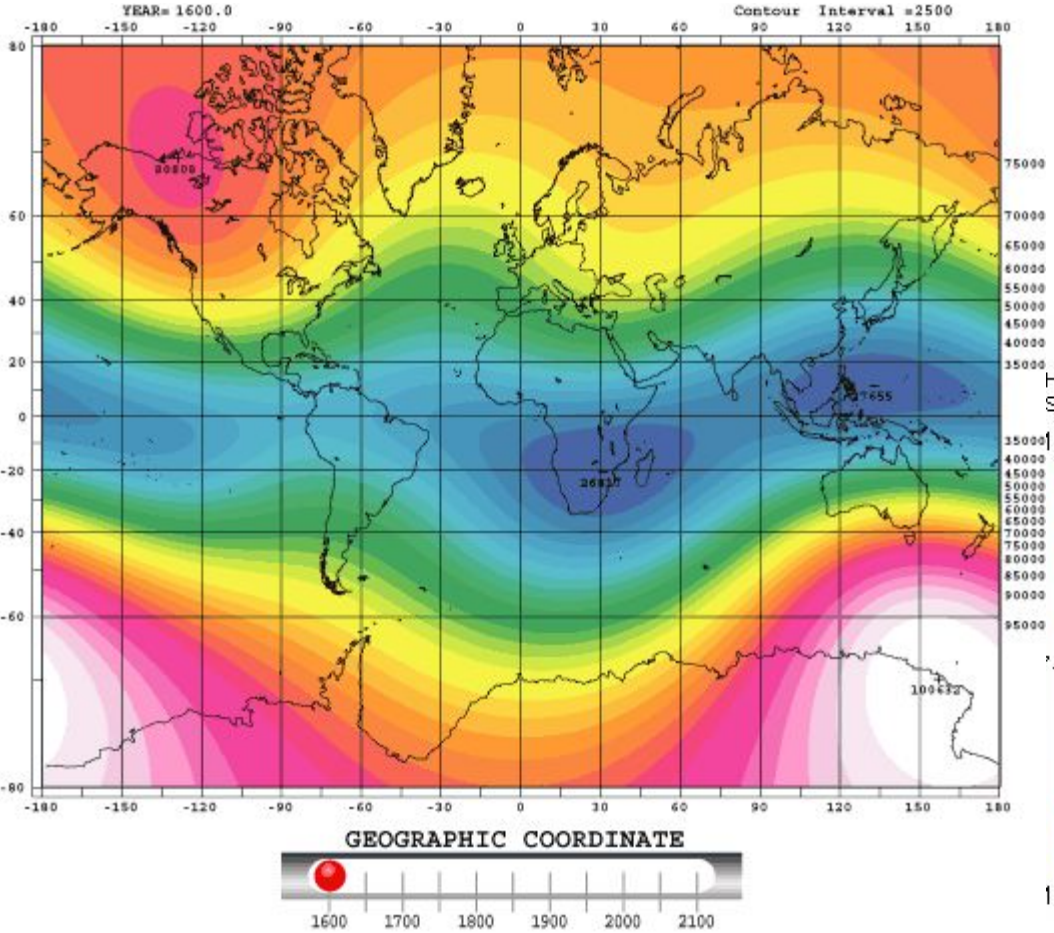

westward drift at a rate of about 0.2 degrees per year

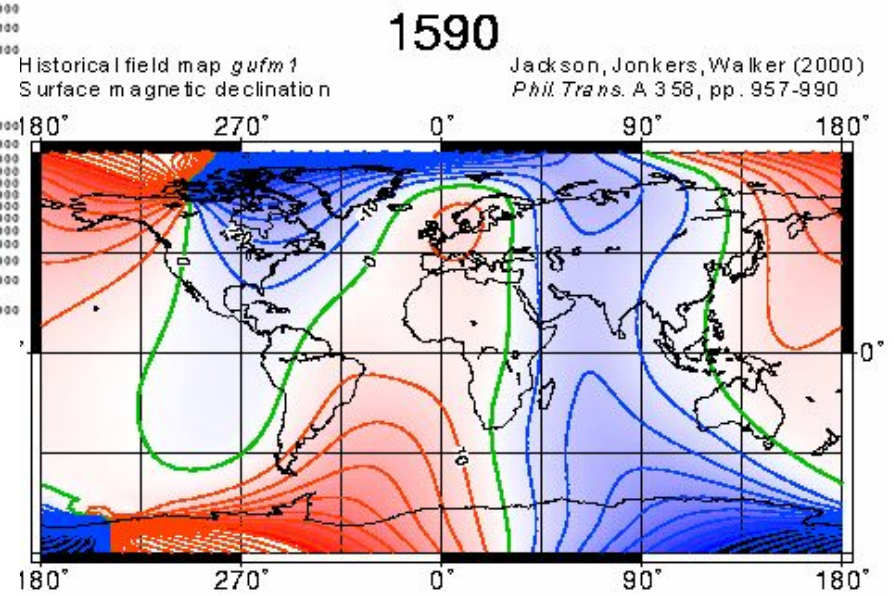

The magnetosphere

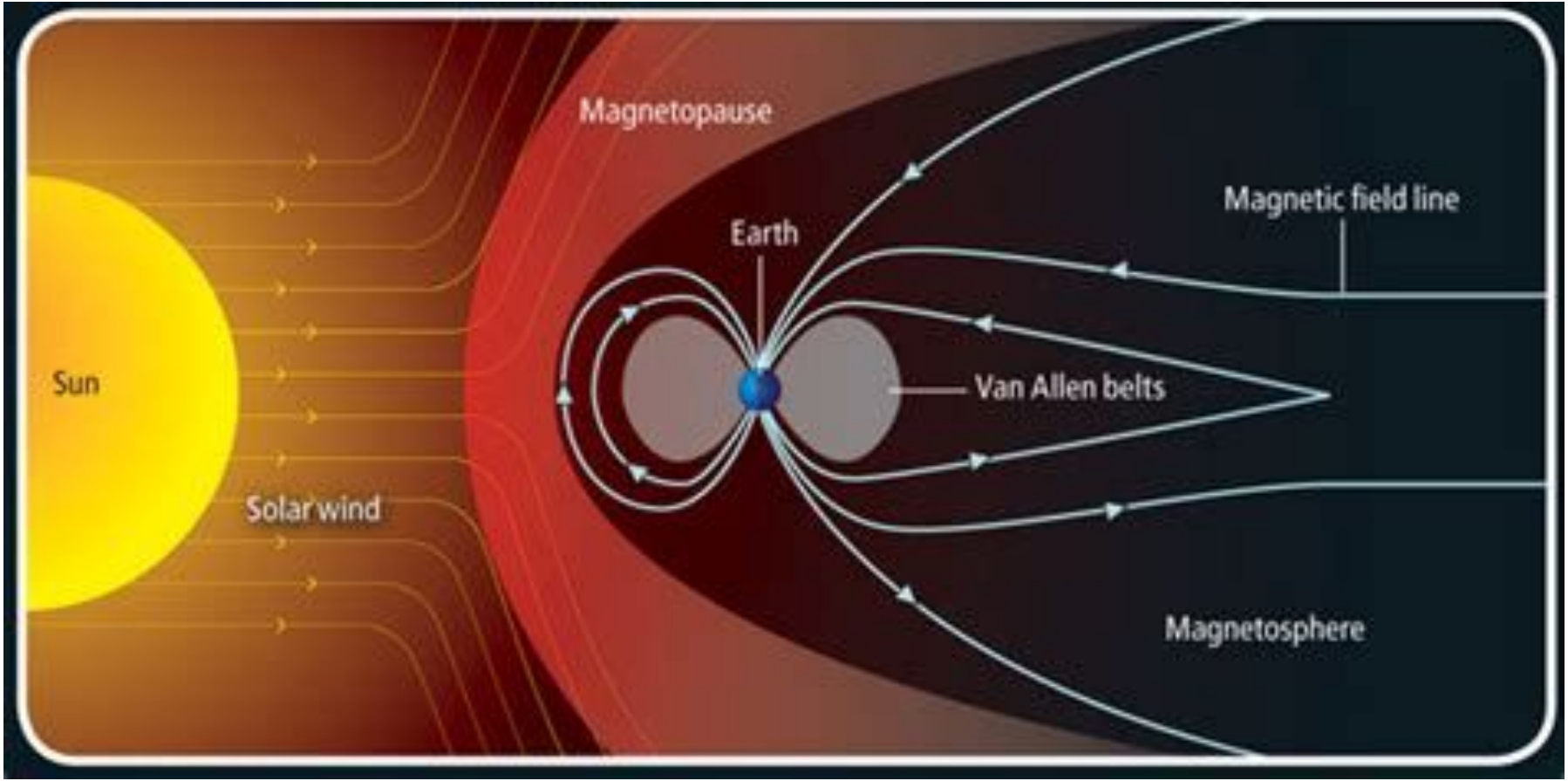

Trapped energetic particles

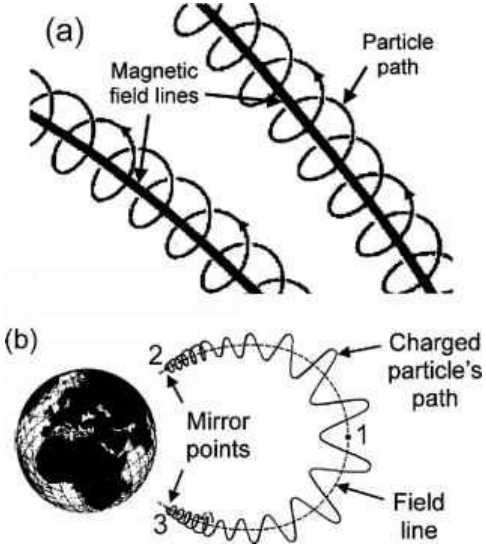

Trapped energetic particles

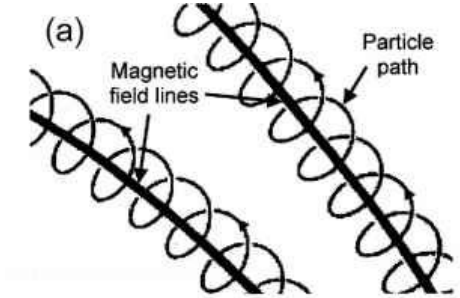

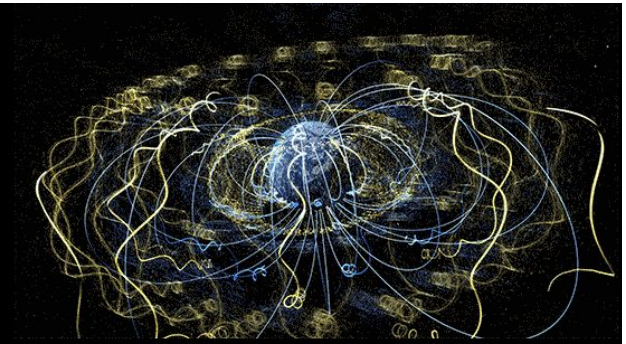

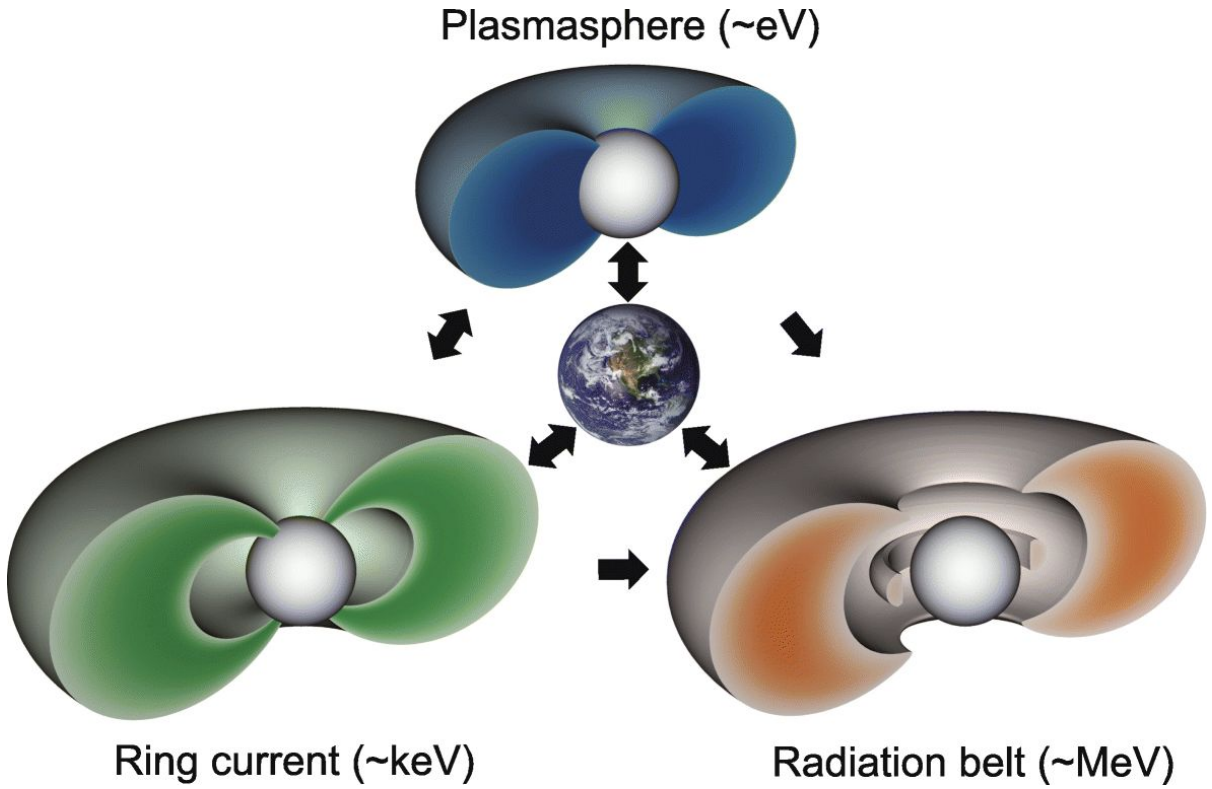

van Allen Radiation Belt

- The outer belt consists mainly of high energy (0.1–10 MeV) electrons trapped by the Earth's magnetosphere.
- It is more variable than the inner belt as it is more easily influenced by solar activity.
- It is almost toroidal in shape, beginning at an altitude of 3 R_E and extending to ten R_E (13,000 to 60,000 km) above the Earth's surface.
- Its greatest intensity is usually around 4–5 R_E.

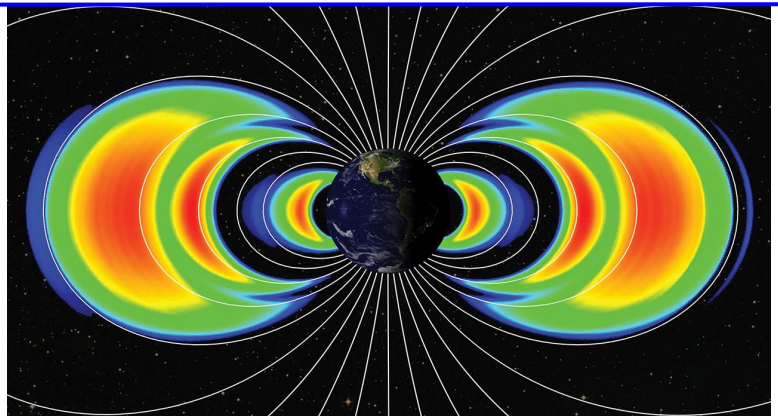

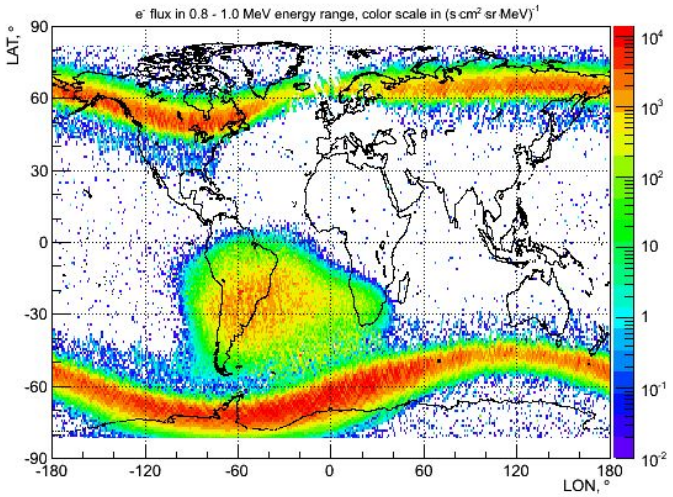

Magnetospheric currents

BTotal = Bp + Ba + Be + Bi

Bp = Main Field (30000 - 60000 nT)

Ba = Magnetization of rocks in the lithosphere (~10-20 nT)

Be = External field related to ionosphere and magnetosphere (10-2000 nT)

Bi = Induced field by external field Be

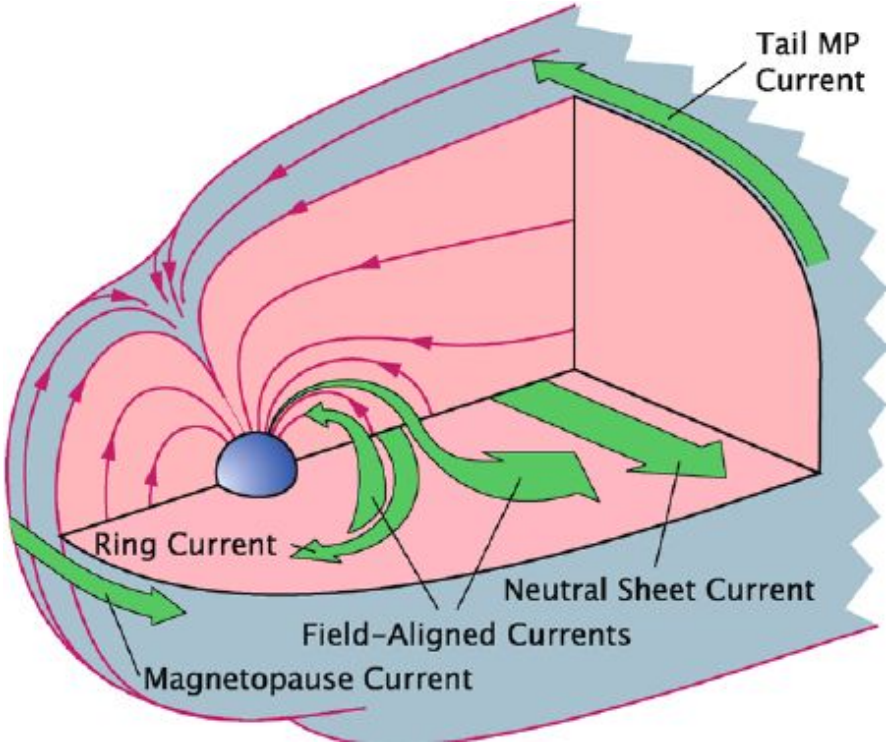

Geomagnetic Storm

Geomagnetic Storms / Substorms → Ionospheric Storms Disturbances/ Instabilities

- HF communications
- GNSS Navigation

Reconnection between interplanetary and Earth's dayside magnetic fields is the basic process for magnetic storms.

A second reconnection on the nightside pushes plasma towards Earth

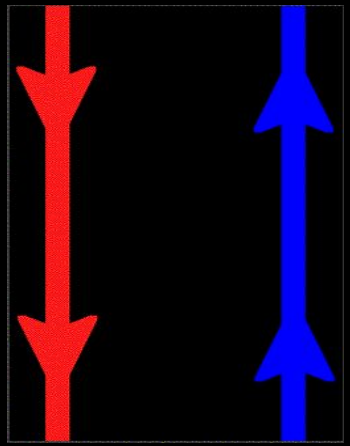

Dst index (Low latitudes)

Main key IP properties (Bs & Vx) determine the level of the geo-storm

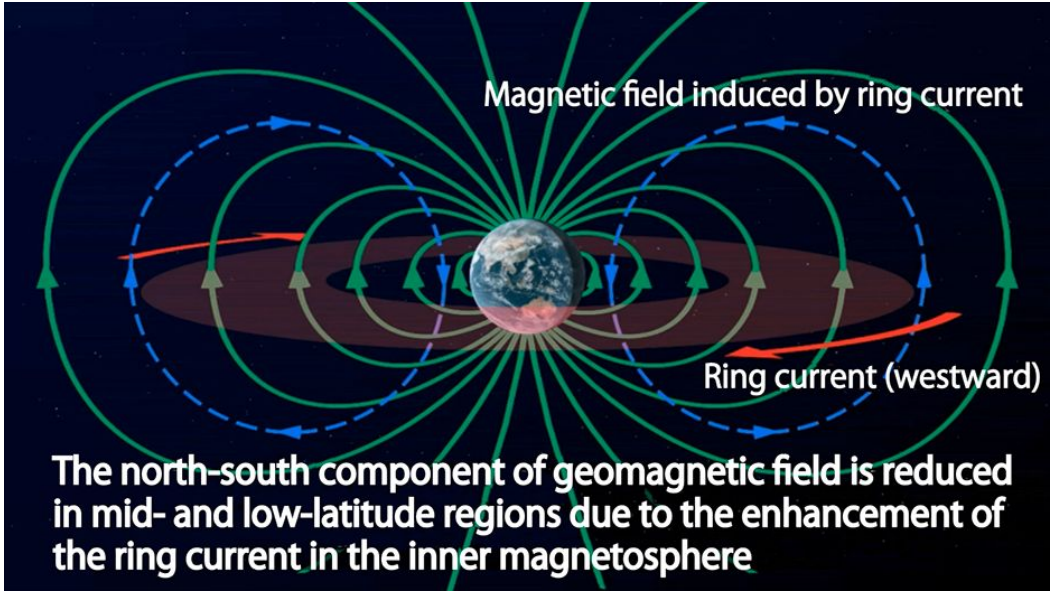

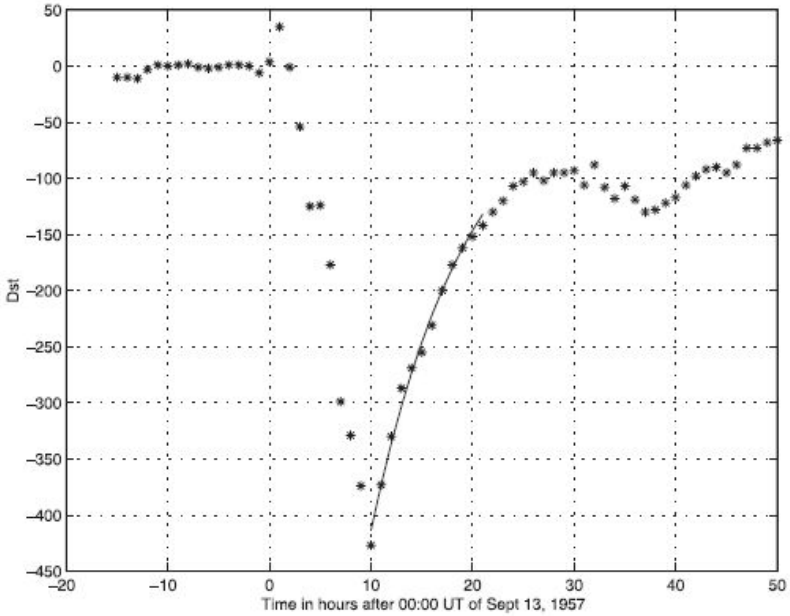

Ring Current: H+, O+, e-
(energies ~keV)

$$dDST/dt + DST/\tau = V_x(t)B_s(t)$$

Burton et al., 1975

Dst index geomagnetic stations

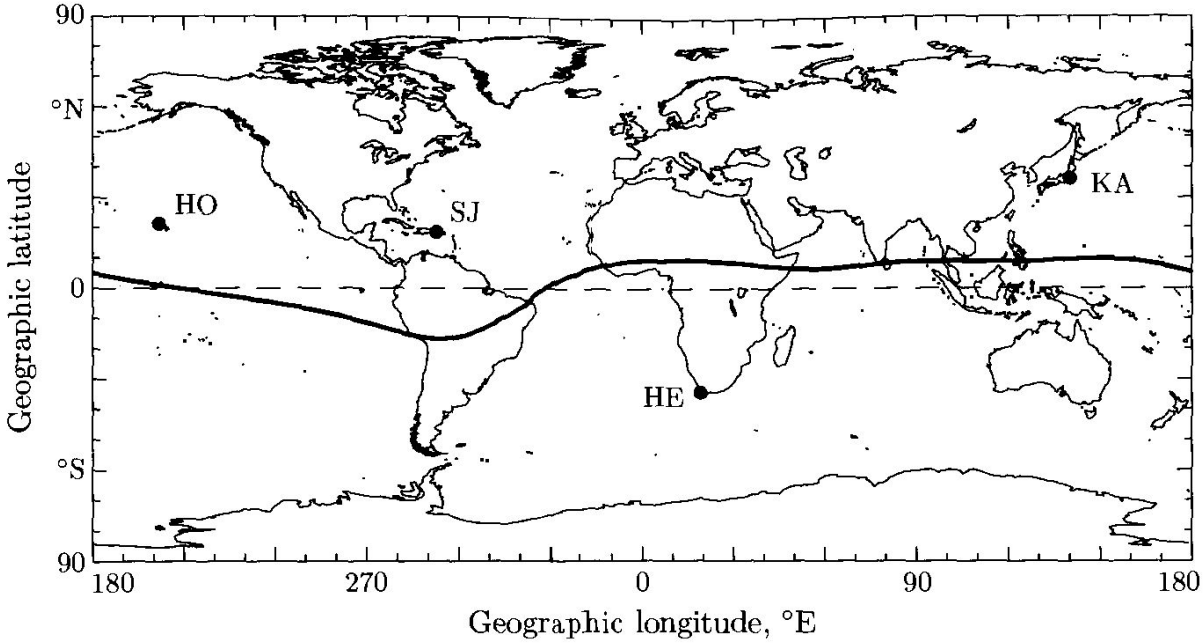

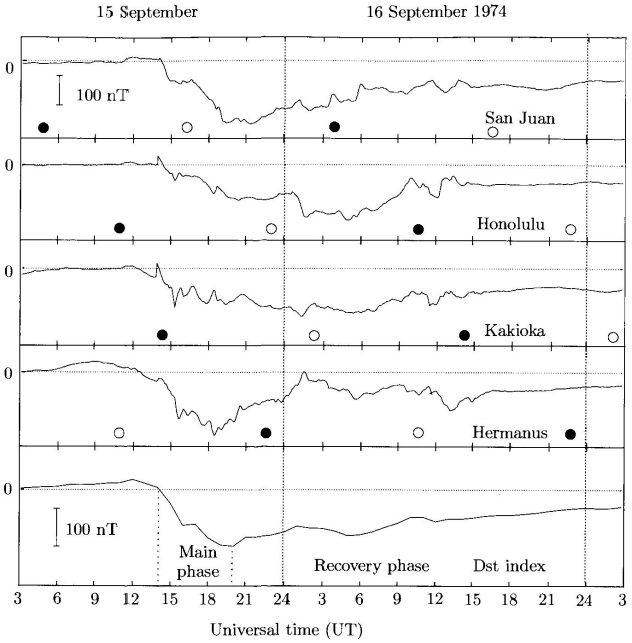

Fig. 8.5. Locations of the magnetic observatories contributing to the Dst index. The abbreviations: HE is Hermanus, KA is Kakioka, HO is Honolulu and SJ is San Juan. The thick solid line indicates the location of the magnetic inclination equator. Note that, in order to minimize the influence of the equatorial electrojet, the stations are located off the magnetic equator.

Kp index (mid latitudes HN) and Ksa index

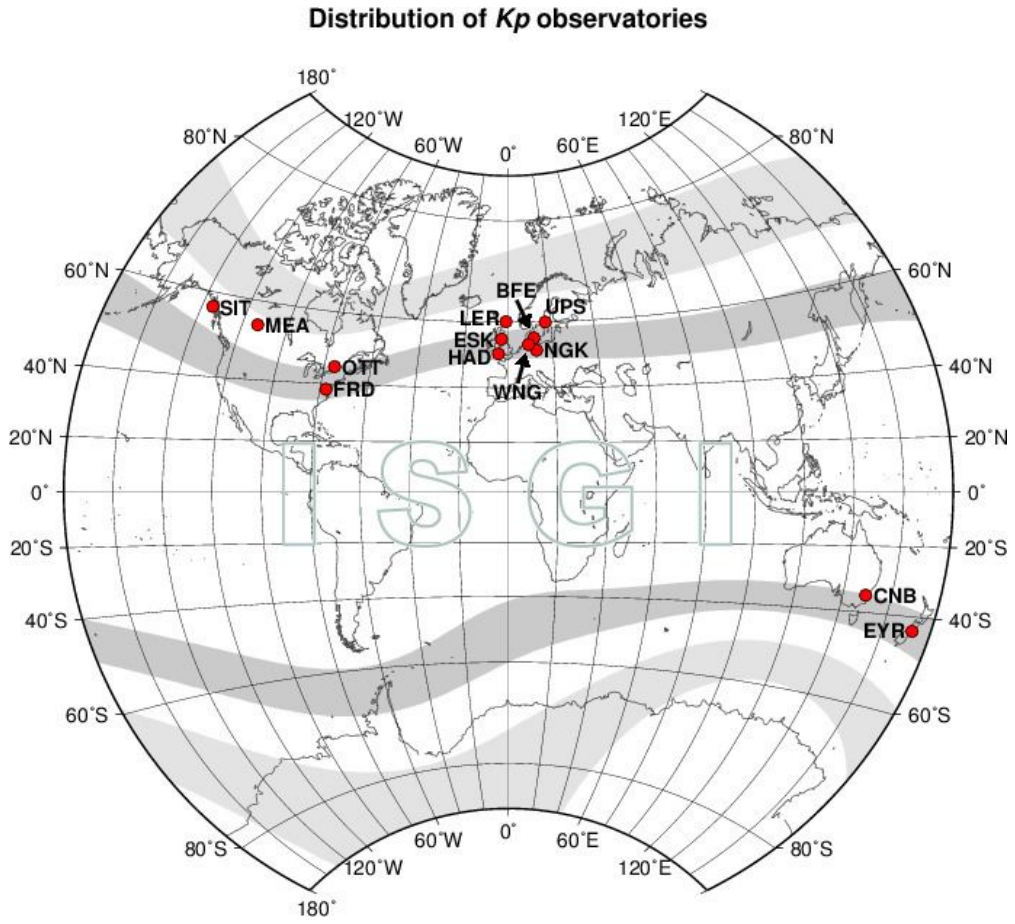

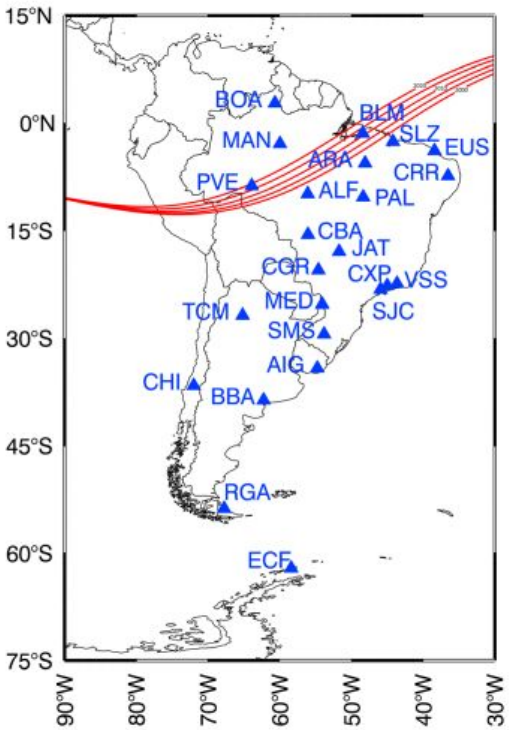

Figure 5. Geographic distribution of the Embrace MagNet stations (and candidate stations) over South America.

Denardini et al (2013, 2018)

Auroral electrojet index (high latitudes)

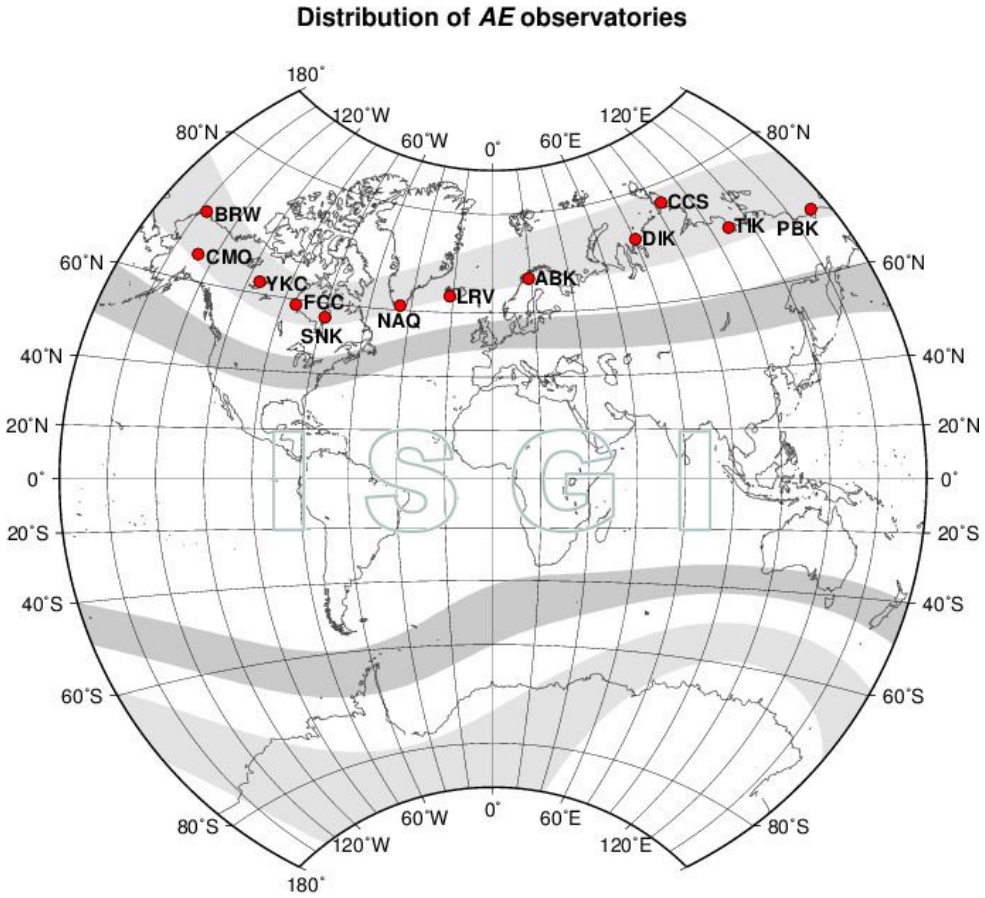

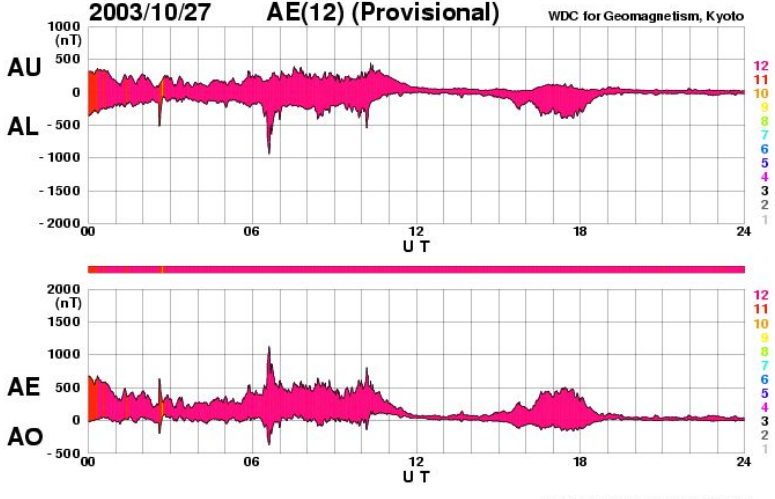

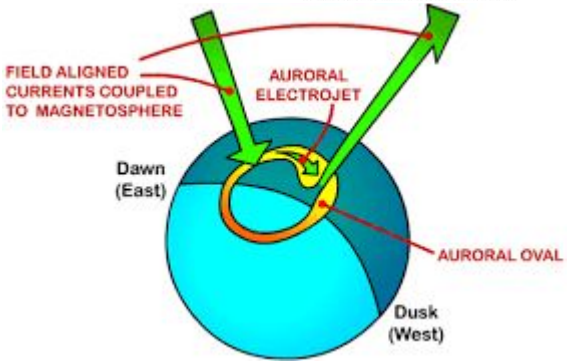

Halloween Geomagnetic Storm

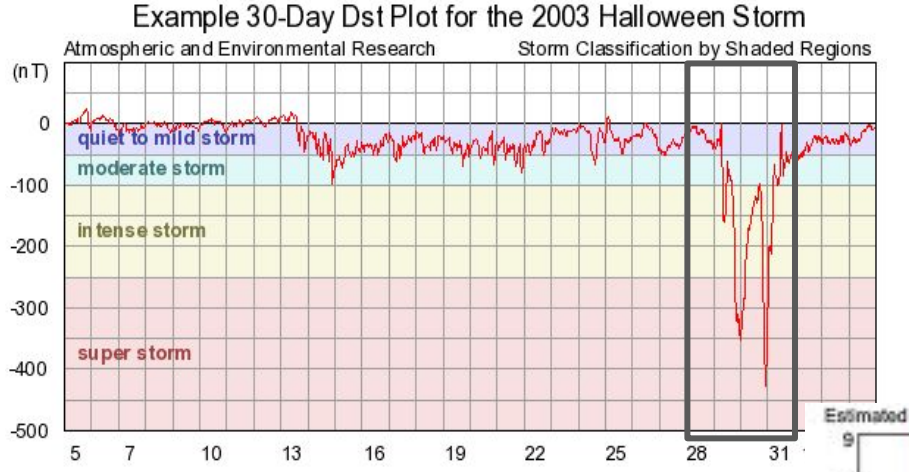

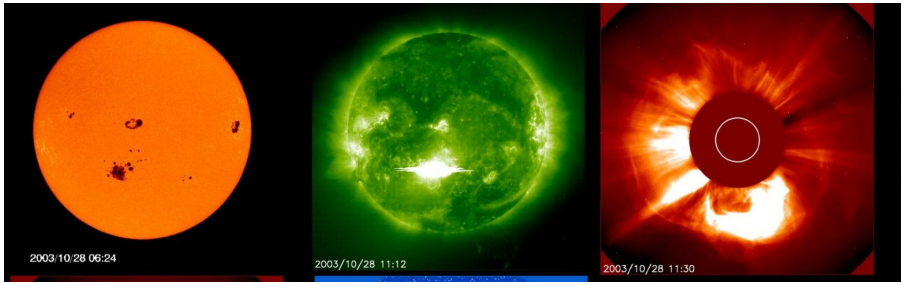

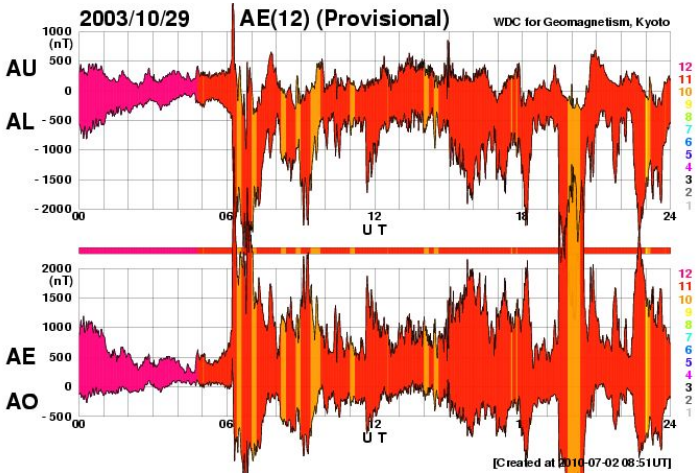

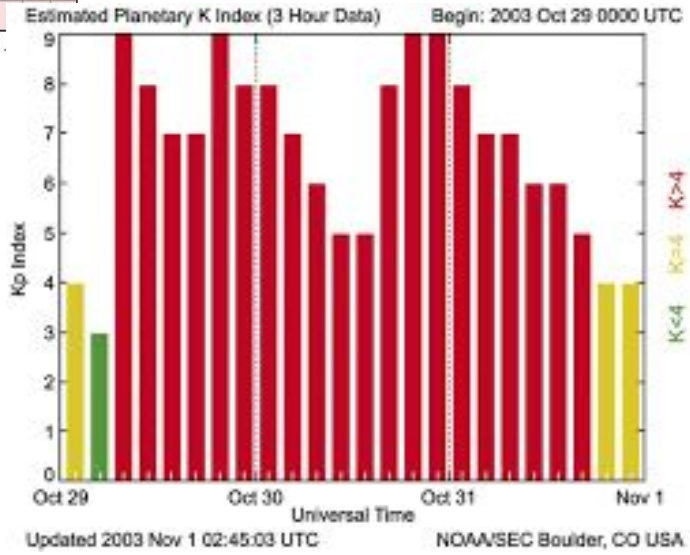

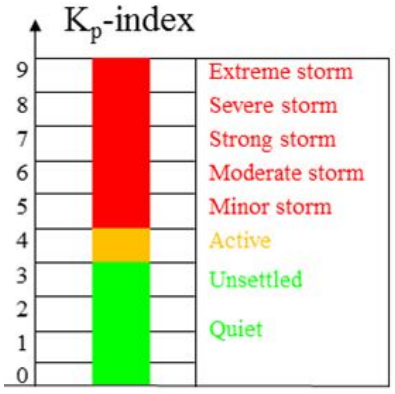

CMEs and Geomagnetic Storms

CMEs

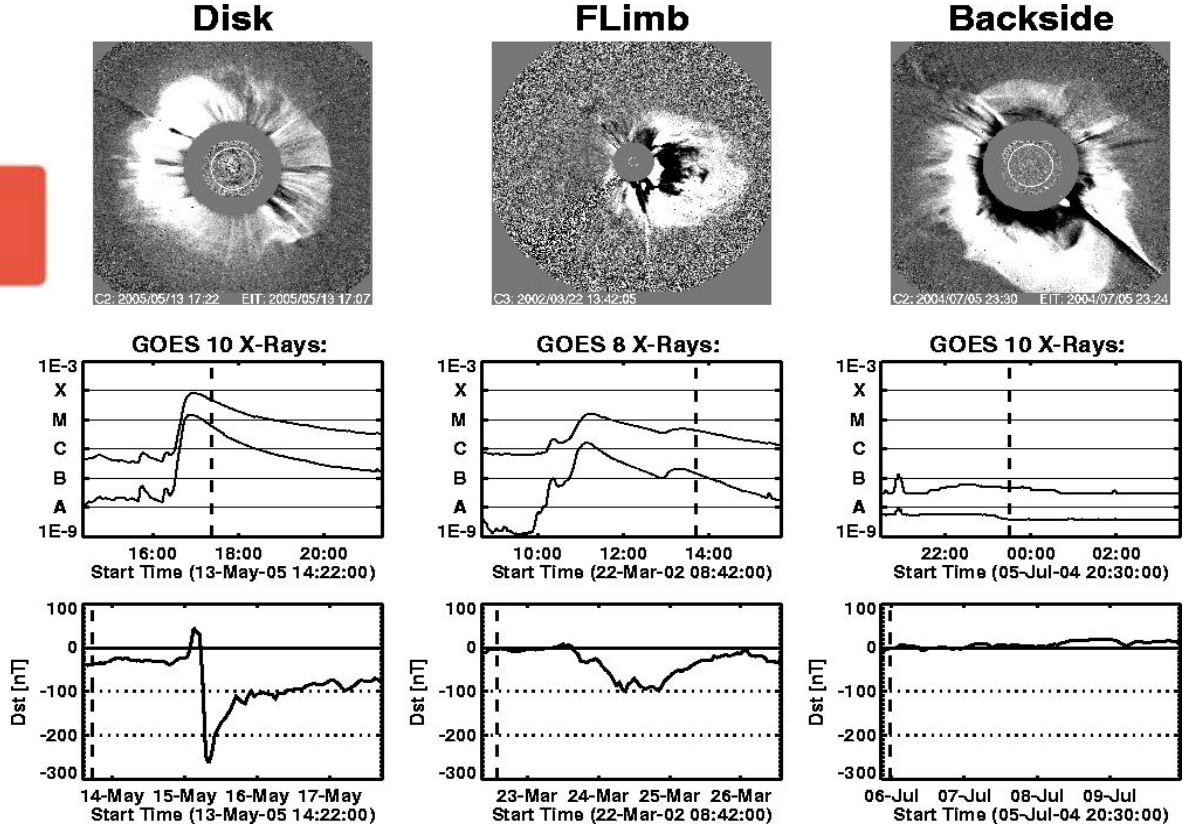

Solar Flare

Geomagnetic Storms / Substorms

Gopalswamy et al. 2007

Direct impact

Glancing impact

No impact

Geomagnetic Storms Impacts

Damage to Electric Power Grids

- Changes in the magnetic field can produce surges in power lines and transformers

Geomagnetic Storms / Substorms

Geomagnetic Storms Impacts

Damage to Electric Power Grids

- Changes in the magnetic field can produce surges in power lines and transformers

Damage to satellites

- Energetic ions can damage solar panels
- increase satellite drag

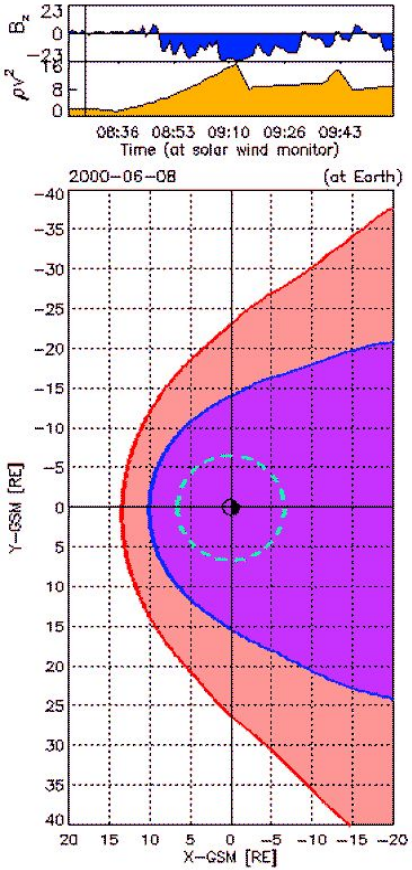

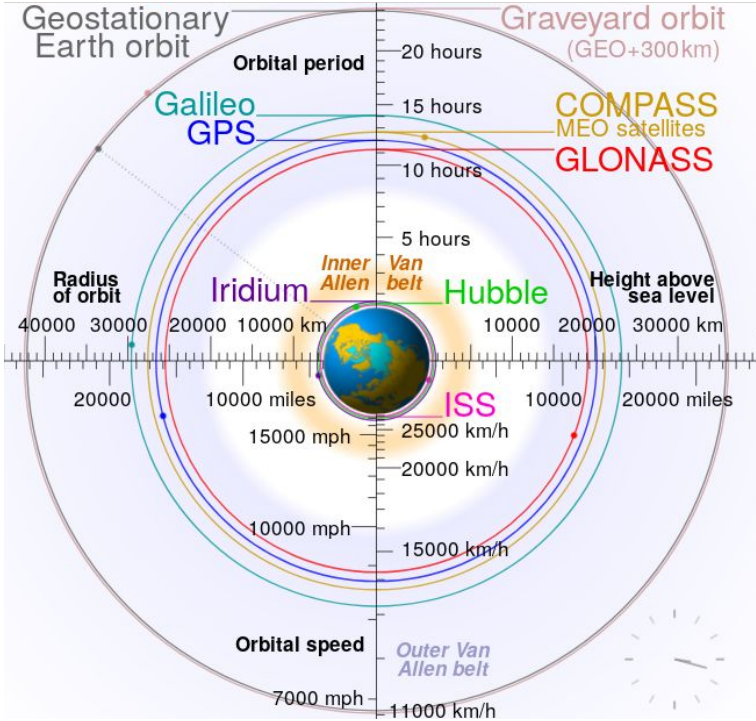

Geomagnetic Storms Impacts

The energetic particles in the radiation belts can impact on satellites, creating a number of hazards to their operation and longevity.

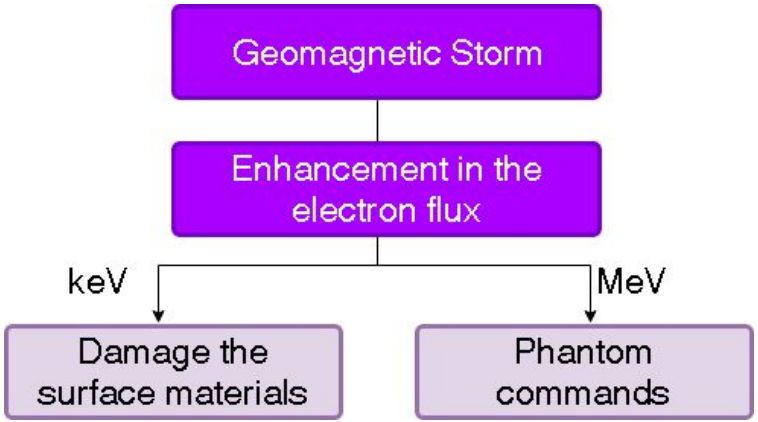

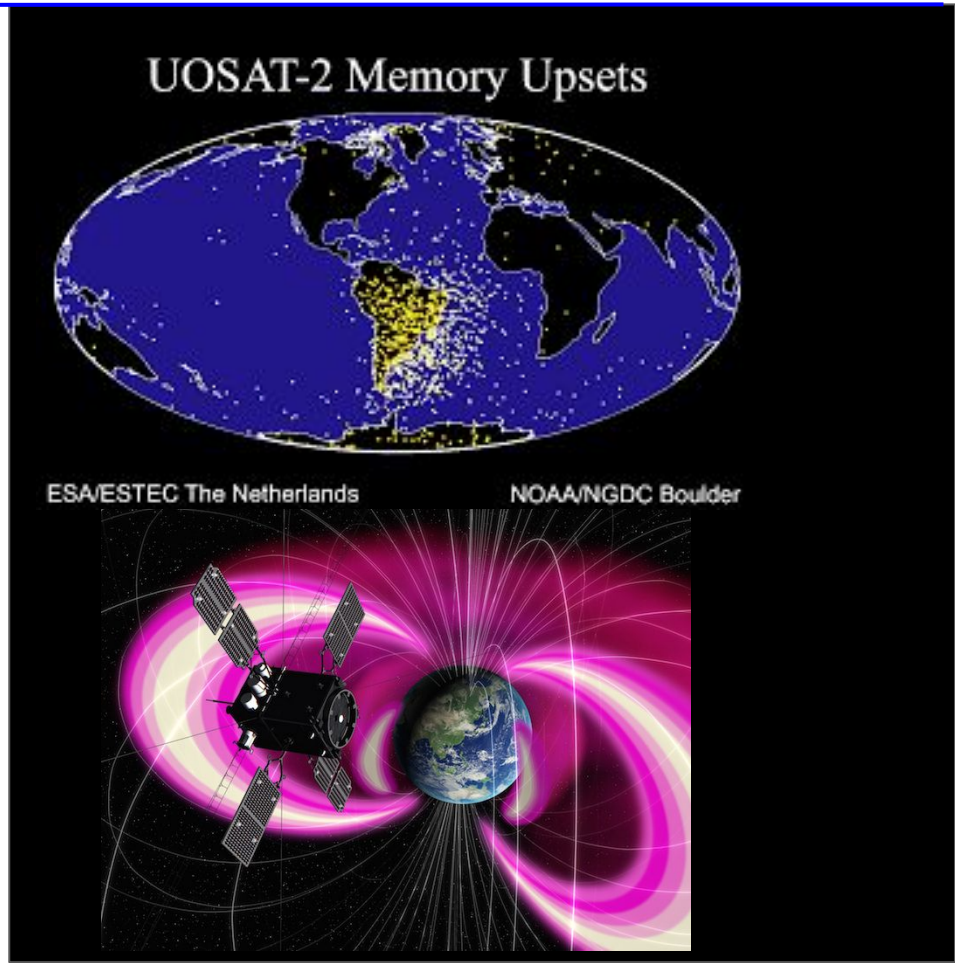

The ionosphere

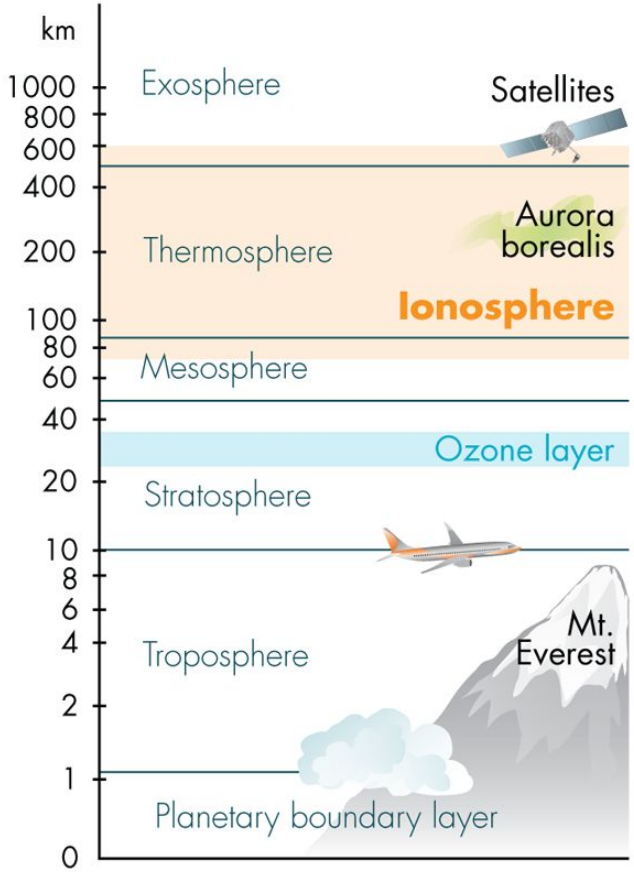

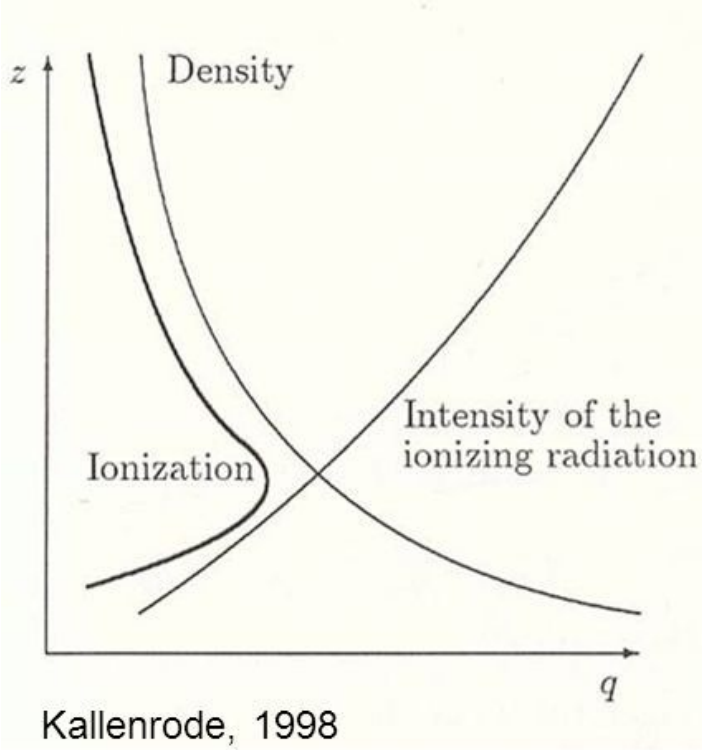

<u>During calm conditions</u>

The density of the ionosphere is less than one percent of the mass of the atmosphere above 100 km.

Solar radiation: EUV, UV, X-ray

Ionospheric and atmospheric composition

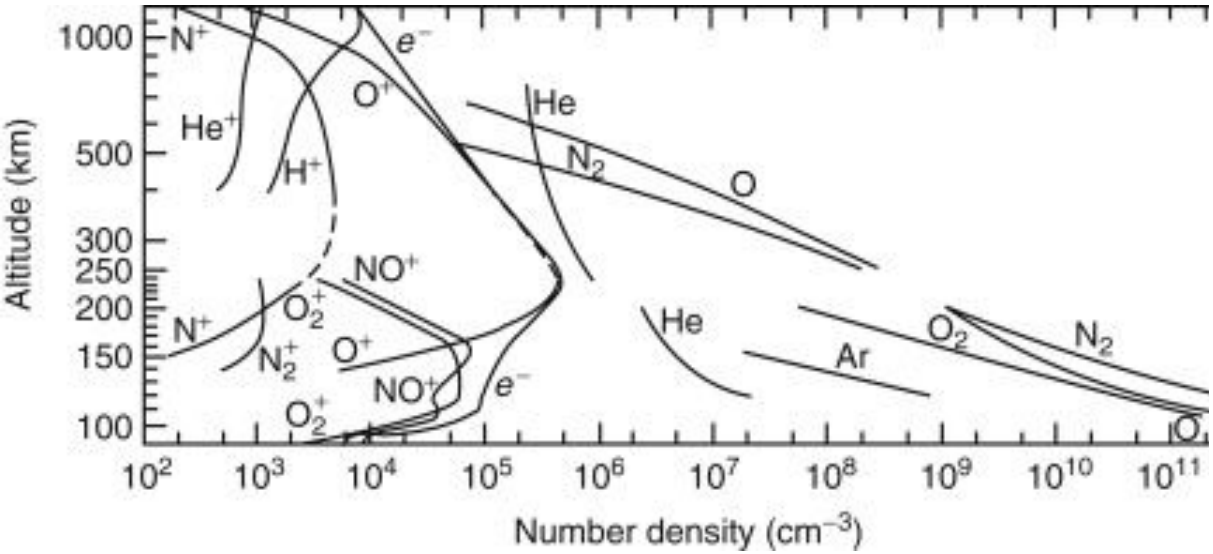

Ion Production/Loss	Reaction
O^+ Production	$O + h\nu \rightarrow O^+ + e$
	$H^+ + O \rightarrow O^+ + H$
O^+ Loss	$O^+ + N_2 \rightarrow NO^+ + N$
	$O^+ + O_2 \rightarrow O_2^+ + O$
	$O^+ + H \rightarrow H^+ + O$
H^+ Production	$O^+ + H \rightarrow H^+ + O$
H^+ Loss	$H^+ + O \rightarrow O^+ + H$
He^+ Production	$He + h\nu \rightarrow He^+ + e$
He^+ Loss	$He^+ + N_2 \rightarrow He + N_2^+$
	$He^+ + N_2 \rightarrow He + N^+ + N$
	$He^+ + O_2 \rightarrow He + O_2^+$

The density of the ionosphere depends on the neutral density and the ionizing radiation

The ionosphere layers

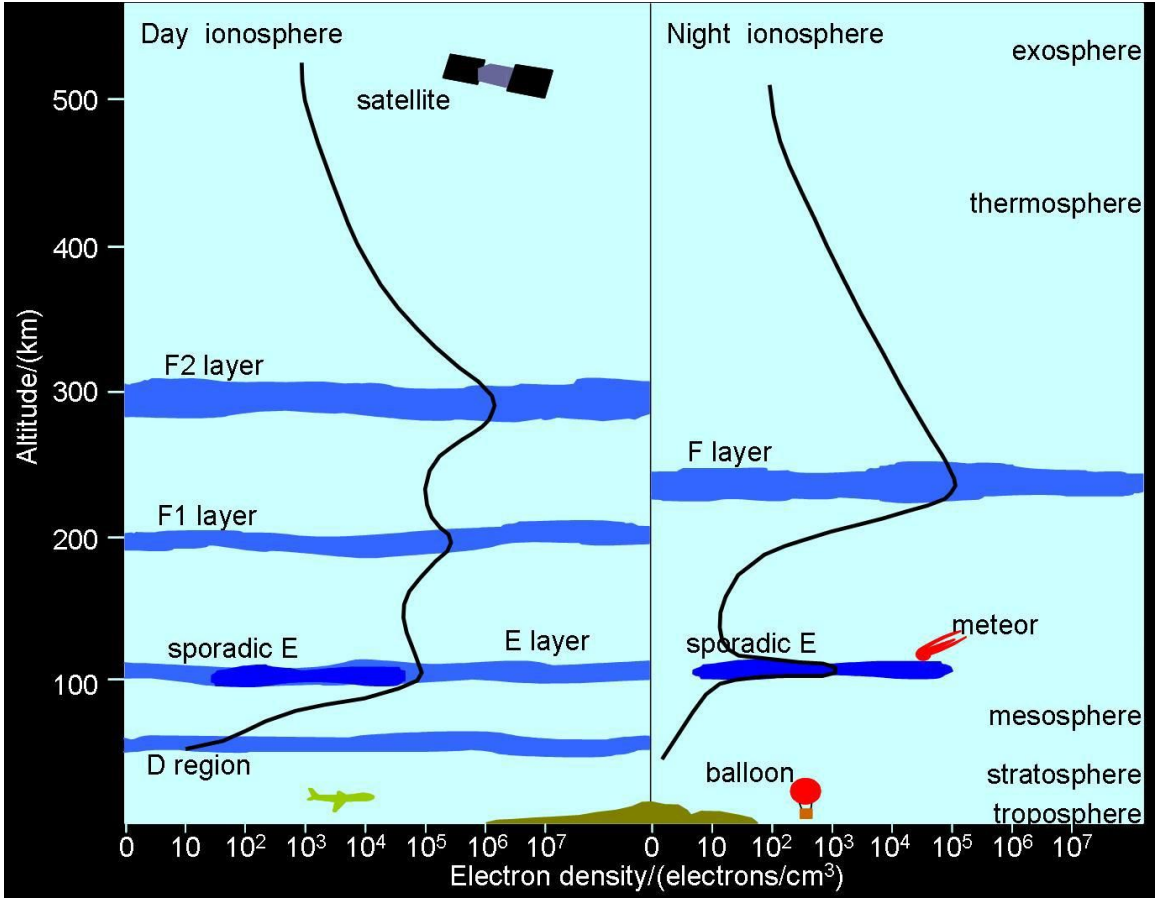

Ionospheric regions and typical daytime electron densities:

- D region: 60–90 km, ne = 10^{8}–10^{10} m^{-3}
- E region: 90–150 km, ne = 10^{10}–10^{11} m^{-3}
- F region: 150–1000 km, ne = 10^{11}–10^{12} m^{-3} .

Ionosphere has great variability:

- Solar cycle variations (in specific upper F region)
- Day-night variation in lower F, E and D regions
- Space weather effects based on short-term solar variability (lower F, E and D regions)

Total Electron Content (TEC)

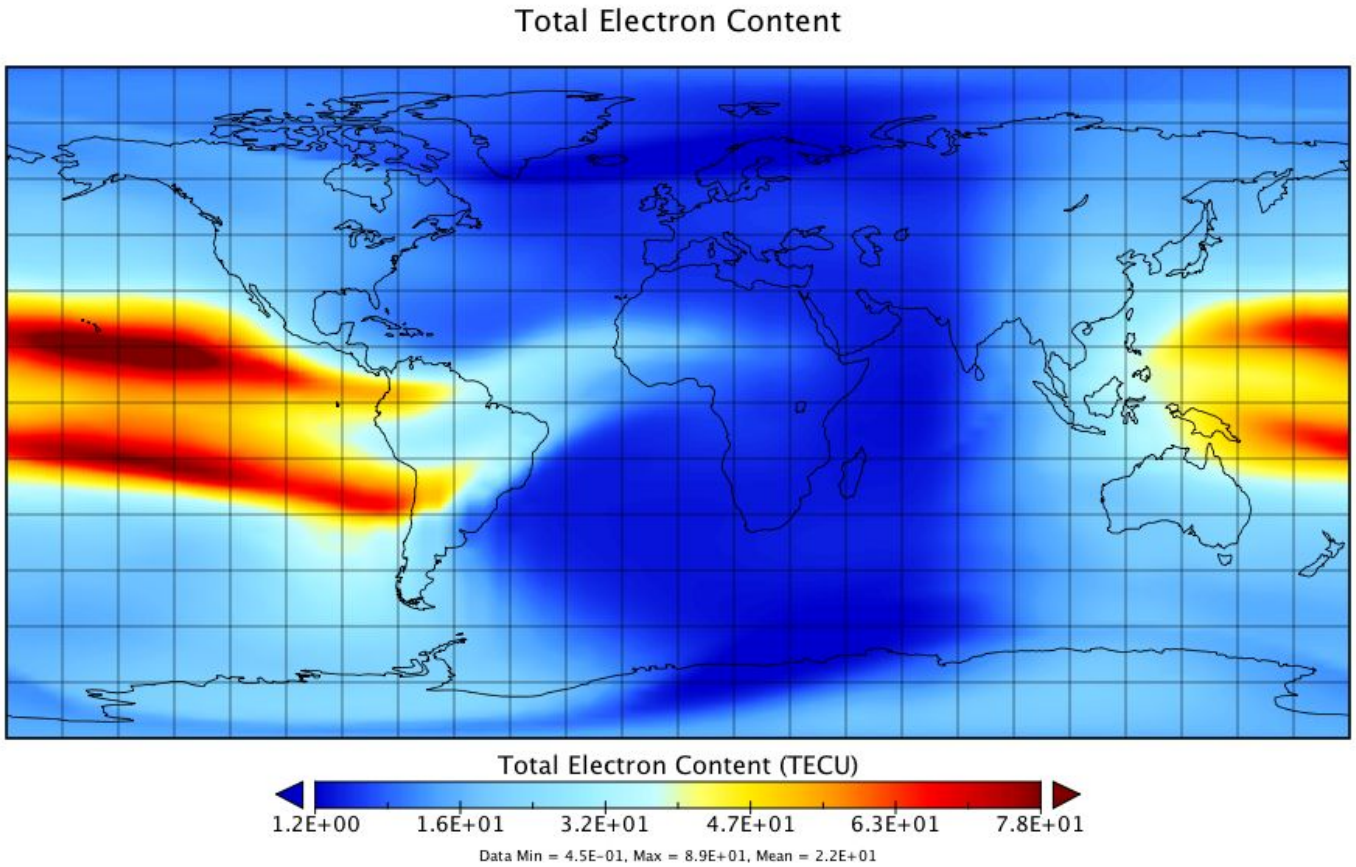

The total electron content (TEC) is defined as the integral of the electron density along the ray path between satellite and receiver.

Thus, TEC provides the number of electrons per square meter. The most frequently used unit is 1TECU = $1x10^{16}$ electrons / m^2.

Equatorial anomaly occurs pre-noon through midnight hours.

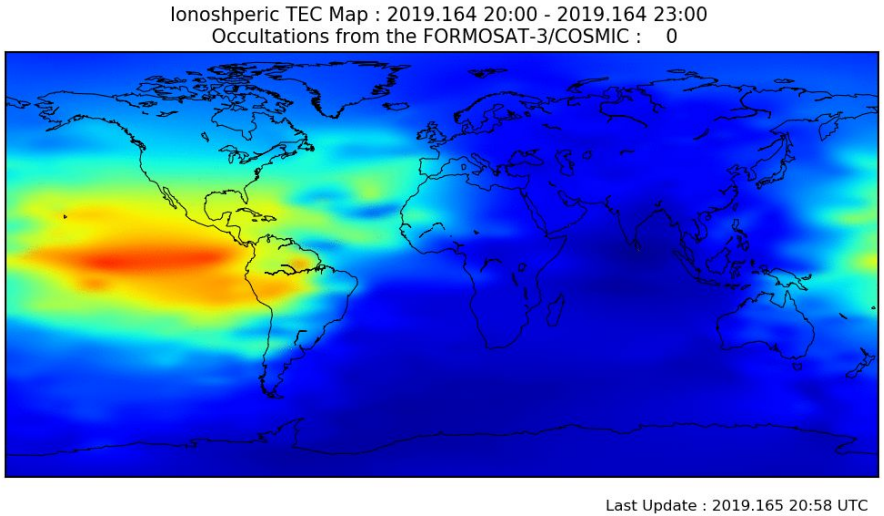

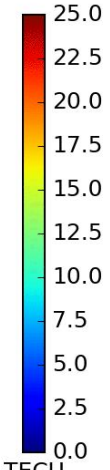

Calm conditions:

Highest values near the equator

Ionospheric storm

Enhancement in TEC

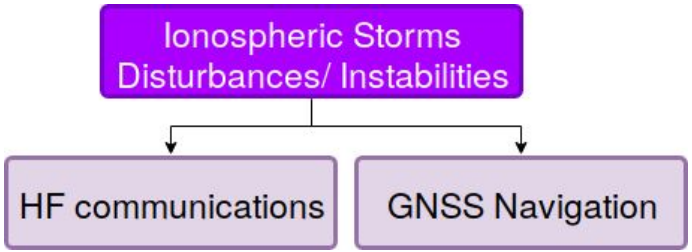

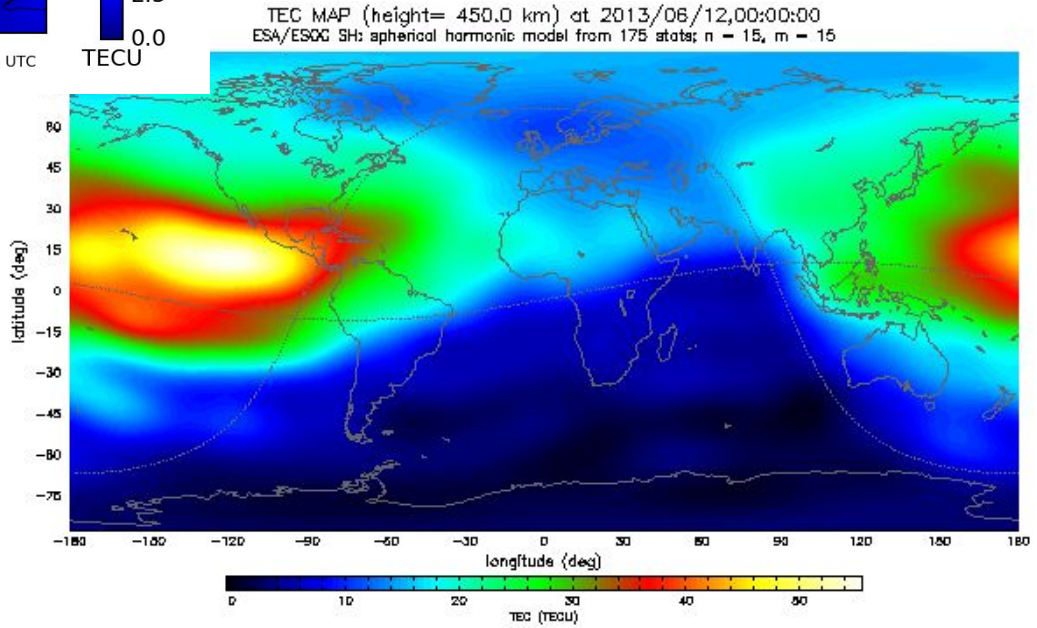

Changes in the density of the F layer

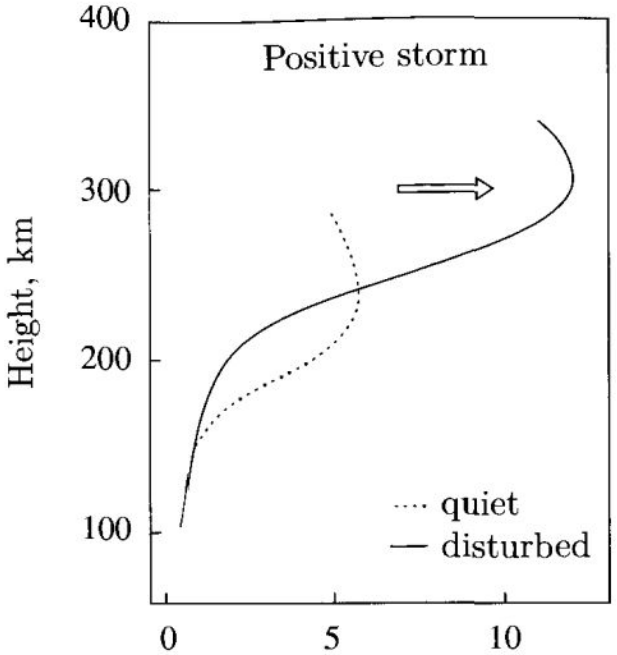

Positive storms: Increase in electron density (mainly in the F layer). Uplift of the F layer.

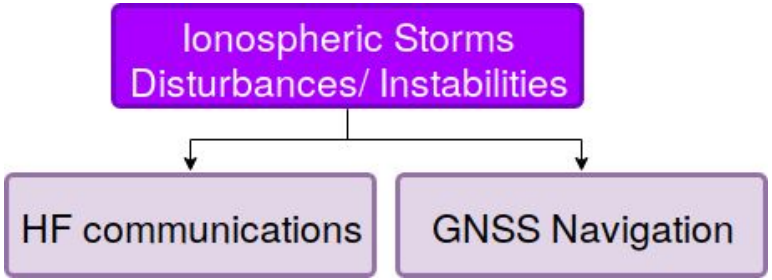

In HF communications is the maximum usable frequency (MUF), which is the maximum frequency reflected by the ionosphere for a given circuit, and is closely related to **foF2**

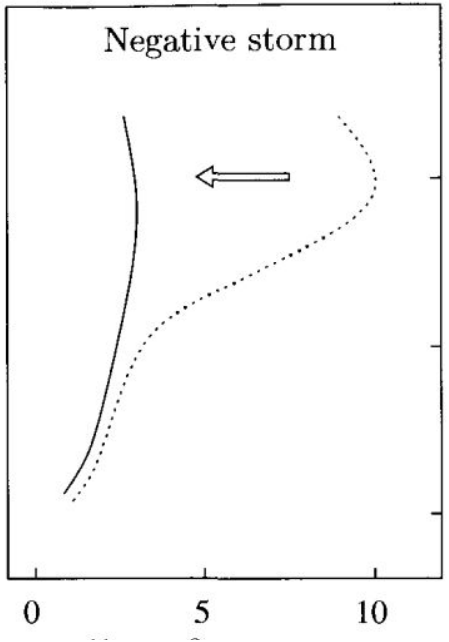

Negative storms: decrease in the electron density.

Ionospheric Scincillation

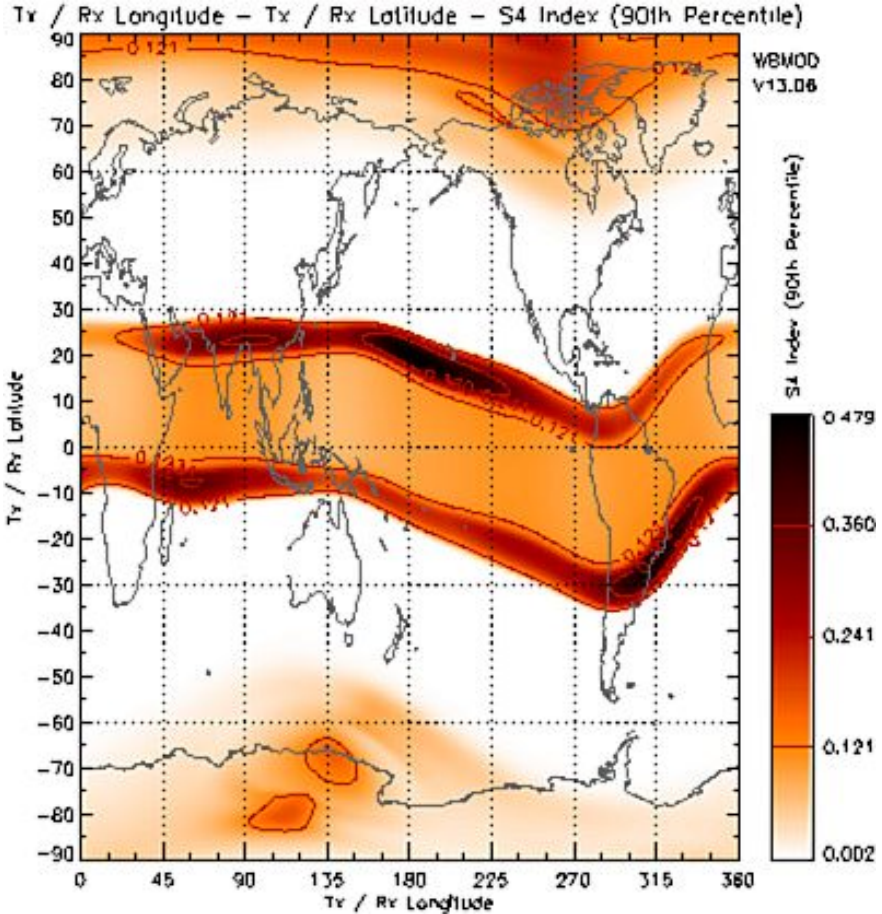

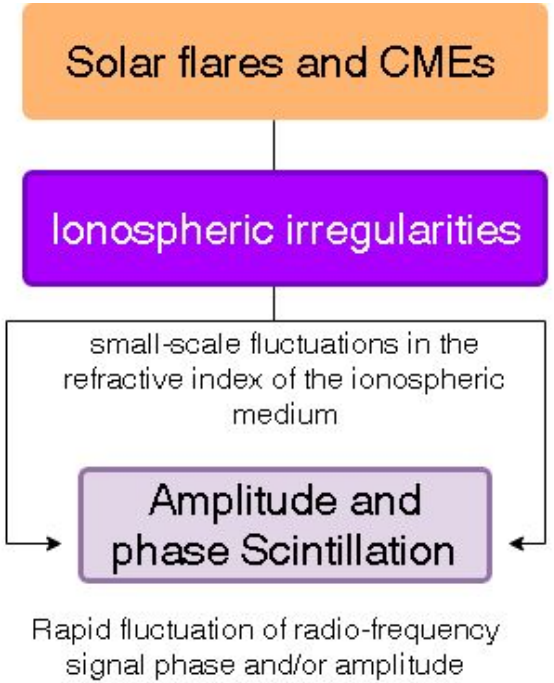

Amplitude scintillation($\mathbf{S_4}$) parameter which is defined as the square-root of the normalised variance of signal intensity over a given interval of time (S4 upper limit of 1.0)

PART II: Space Weather Impacts

Damage to communication

- Radio interference
- Reduced accuracy of GNSS
- Radio emissions during flares reduces signal-to-noise

Affect all GNSS applications

- Geologic Exploration
- Continental Cables
- Fiber Optic Cable
- Surveillance
- Banking
- Remote sensing
- Emergency Location
- Natural Resource Monitoring
- All modes of transportation

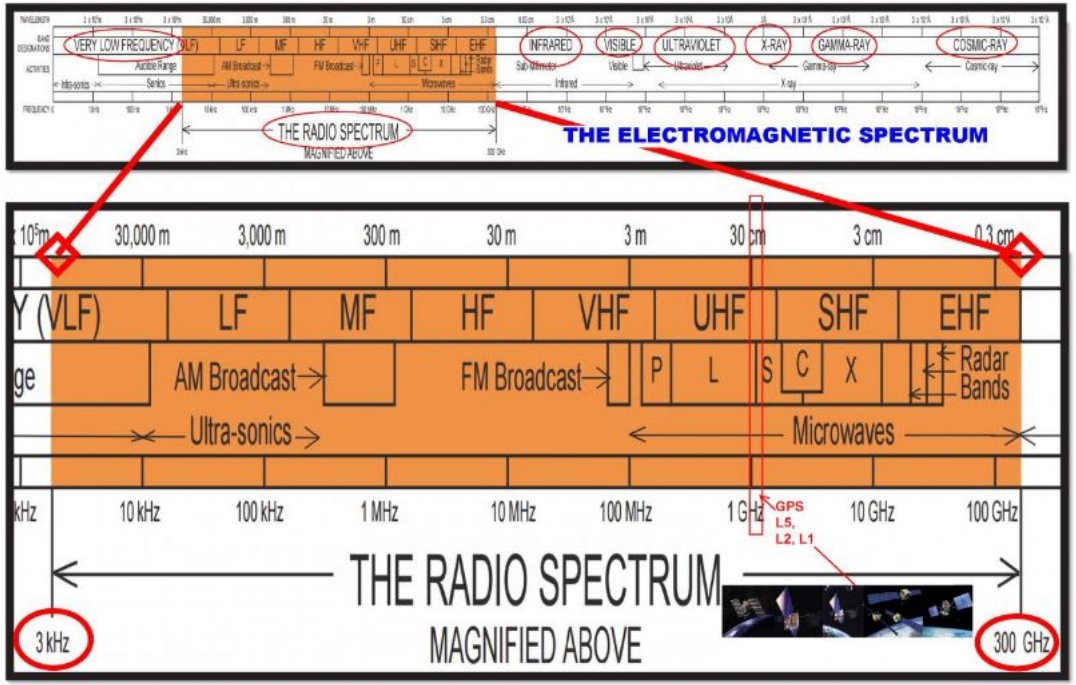

Summary

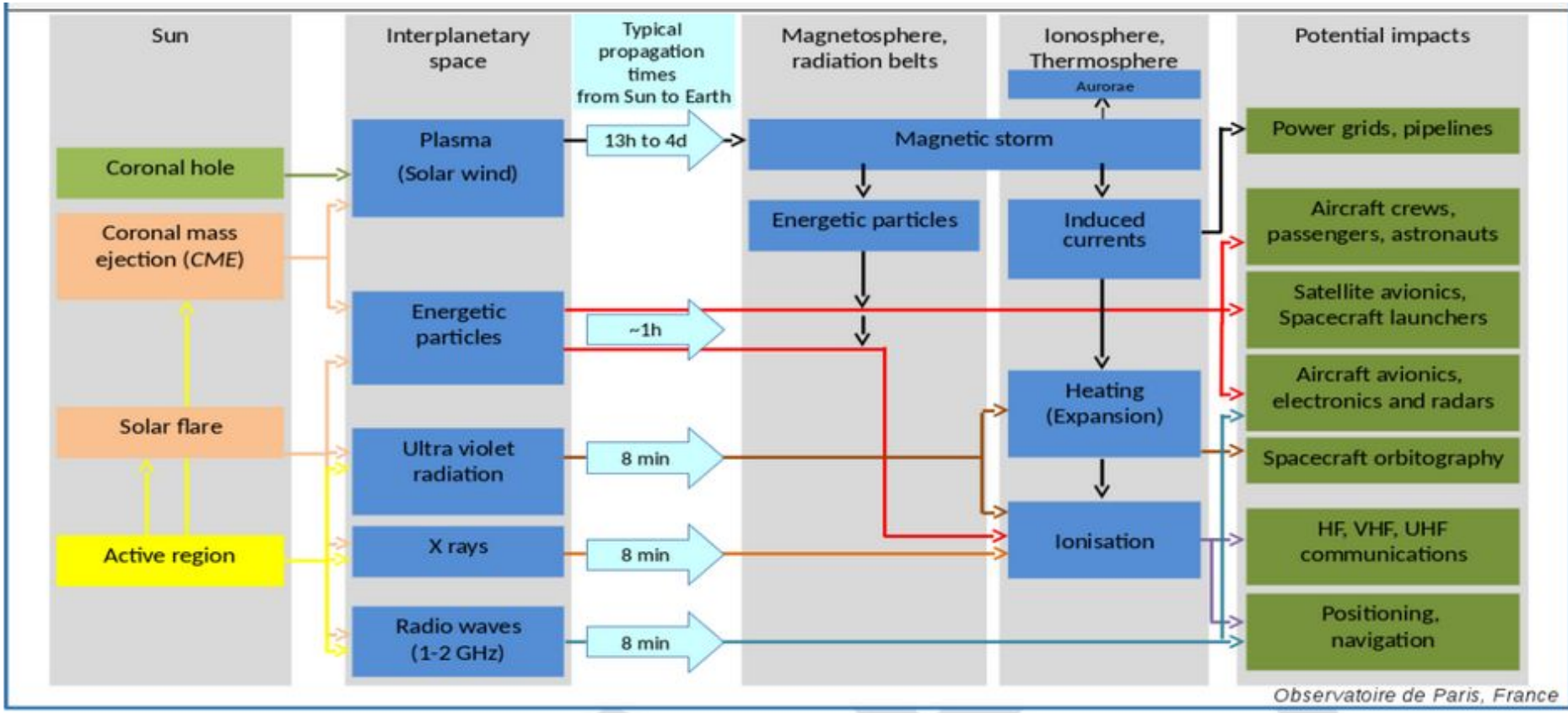
Sun
Interplanetary space
Typical propagation times from Sun to Earth
Magnetosphere, radiation belts
Ionosphere, Thermosphere
Aurorae
Potential impacts
Coronal hole
Coronal mass ejection (CME)
Solar flare
Active region
Plasma (Solar wind)
Energetic particles
Ultra violet radiation
X rays
Radio waves (1-2 GHz)
13h to 4d
~1h
8 min
8 min
8 min
Magnetic storm
Energetic particles
Induced currents
Heating (Expansion)
Ionisation
Power grids, pipelines
Aircraft crews, passengers, astronauts
Satellite avionics, Spacecraft launchers
Aircraft avionics, electronics and radars
Spacecraft orbitography
HF, VHF, UHF communications
Positioning, navigation
Observatoire de Paris, France

What can we say about the modern maximum?

Extreme geomagnetic storms recorded (since 1932…)

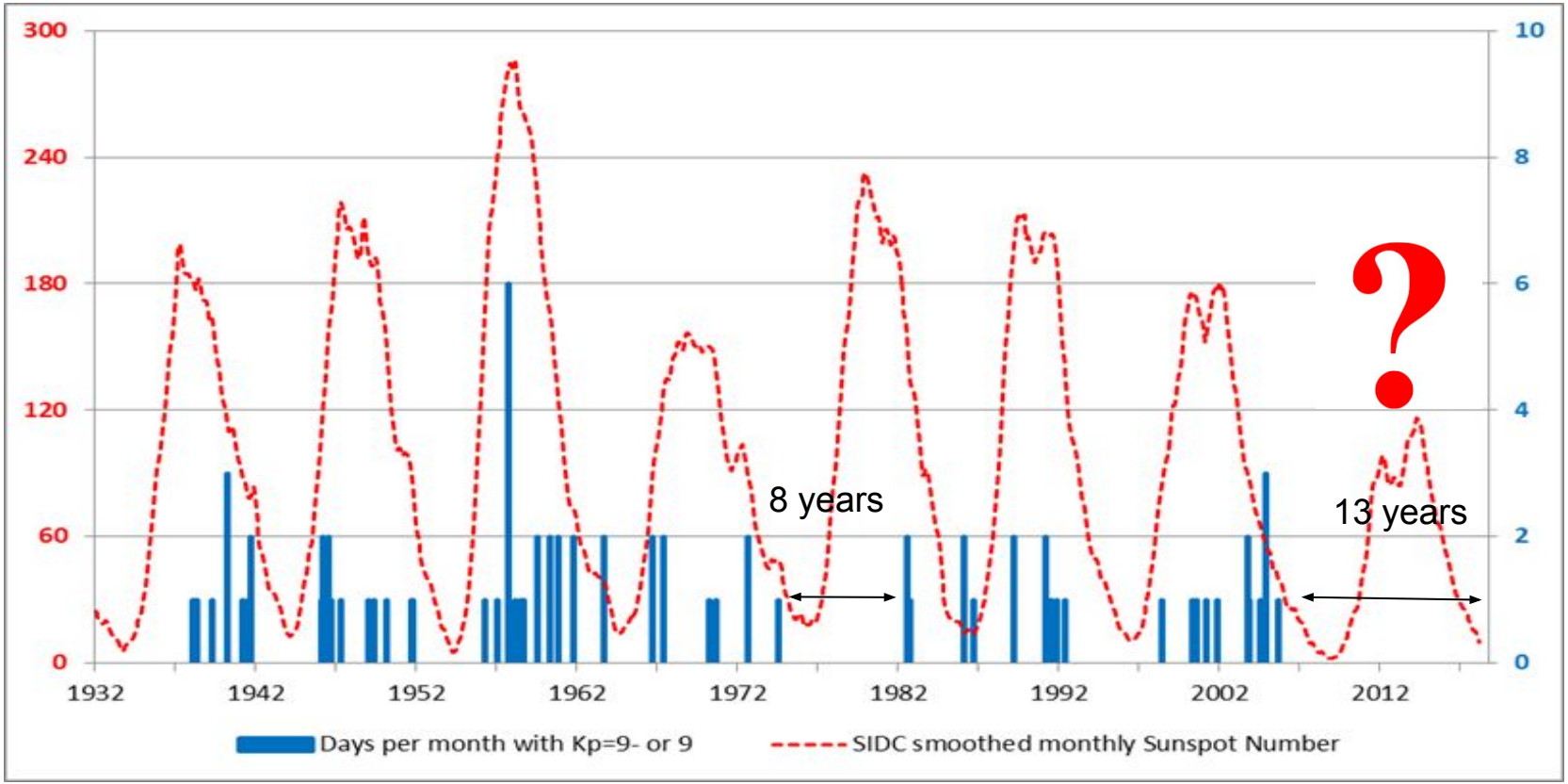

http://www.stce.be/news/441/welcome.html

Massive CME July 23, 2012

Geomagnetic Storms / Substorms

nature COMMUNICATIONS

Article | Published: 18 March 2014

Observations of an extreme storm in interplanetary space caused by successive coronal mass ejections

Ying D. Liu ✉, Janet G. Luhmann, Primož Kajdič, Emilia K.J. Kilpua, Noé Lugaz, Nariaki V. Nitta, Christian Möstl, Benoit Lavraud, Stuart D. Bale, Charles J. Farrugia & Antoinette B. Galvin

Nature Communications **5**, Article number: 3481 (2014) | Download Citation ⬇

Estimations:

- **Dst of -1200** (comparable to the Carrington Event and twice as bad as the March 1989 Quebec blackout.")

  Baker(2013)

- Transit time for the **shock front** of less than **19 h.**
- **2 h** later, the **leading edge of the magnetic cloud**
- A peak **solar wind** speed of **2246 km/s**
- A peak **total magnetic field of 109 nT**

  Cash et. al (2015)

Massive CME July 23, 2012

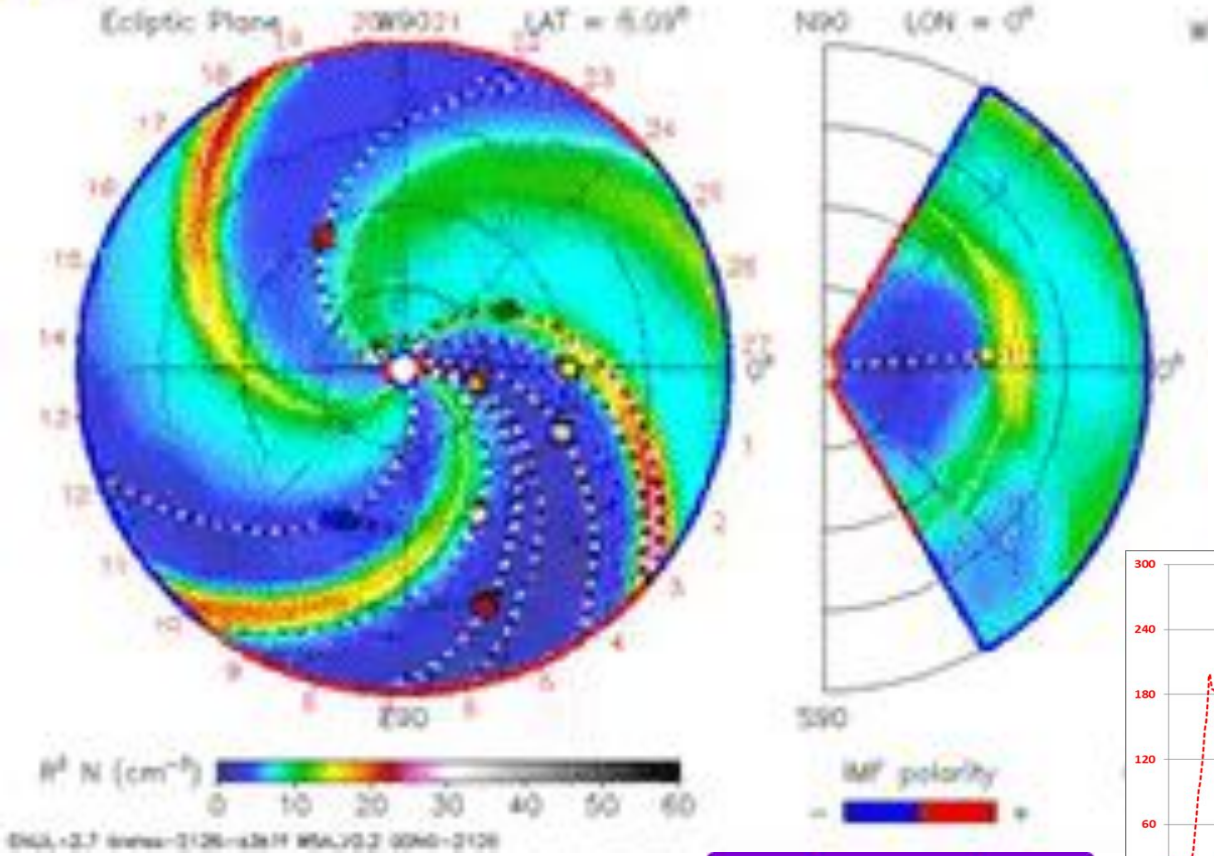

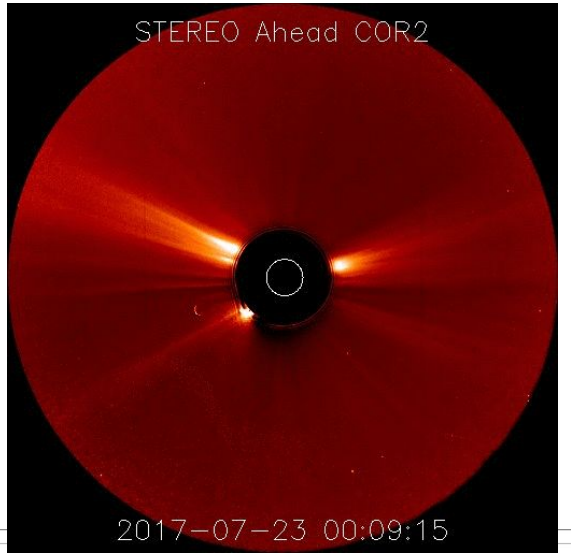

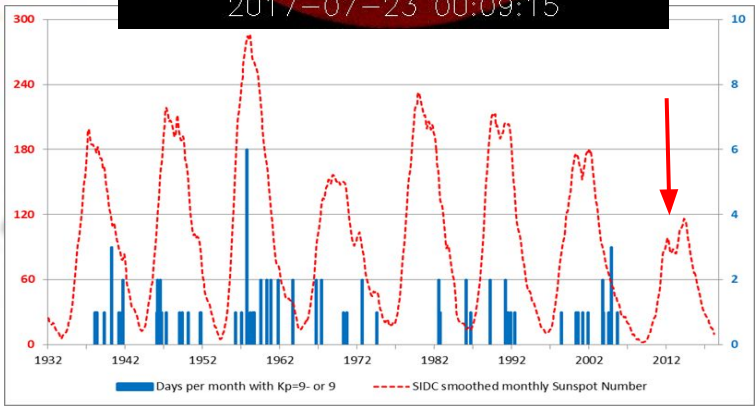

Geomagnetic Storms / Substorms

Solar Cycle 25 predictions

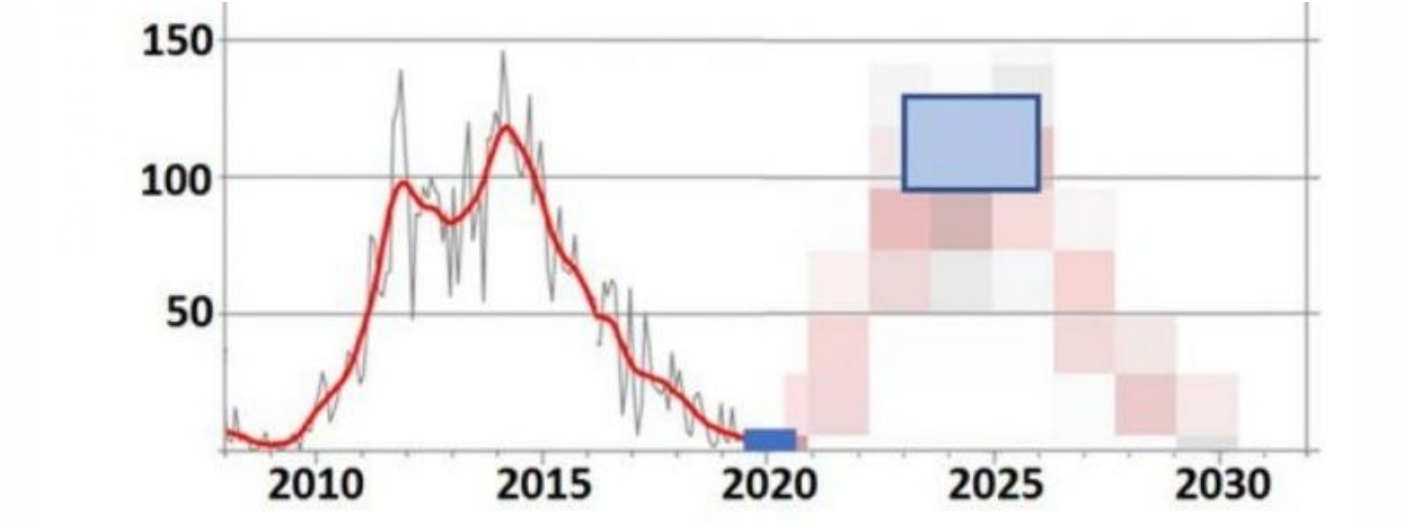

The consensus: Cycle 25 will be similar in size to cycle 24. It is expected that **sunspot maximum** will occur no earlier than the year **2023** and no later than **2026** with a minimum peak sunspot number of 95 and a maximum of 130.

https://www.swpc.noaa.gov/news/solar-cycle-25-preliminary-forecast

Preguntas